Monod parameterization and competition at low iron among freshwater cyanobacteria and chlorophytes

Purnank Shah[1], Shelley K. McCabe[2], Jason J. Venkiteswaran[1], Lewis A. Molot[3], Sherry L. Schiff[4]

1. Department of Geography and Environmental Studies, Wilfrid Laurier University, Ontario, Canada
2. Department of Biology, York University, Toronto, Ontario, Canada
3. Faculty of Environmental and Urban Change, York University, Toronto, Ontario, Canada
4. Department of Earth and Environmental Sciences, University of Waterloo, Waterloo, Ontario, Canada

Correspondence

Lewis A. Molot, Faculty of Environmental and Urban Change, York University, Toronto, Ontario, Canada, M3A 3L4

Email: lmolot@yorku.ca

Abstract

1. This study combines two approaches to explore the utility of Monod growth kinetics to predict competition outcomes between freshwater cyanobacteria and chlorophytes at low iron Fe. Fe threshold concentrations (Fe_T) below which growth ceases, and growth affinities (slope of Fe concentration vs growth rate near Fe_T) were estimated for three large-bodied cyanobacteria (two N-fixers and *Microcystis*) and two chlorophytes in batch cultures.
2. Mean Fe_T for N-replete cyanobacteria, N-deplete (when N-fixing) cyanobacteria and chlorophytes were 0.076, 0.736 and 0.245 nmol L^{-1}, respectively. Mean affinities were 0.937, 0.597 and 0.412 L $nmol^{-1}$ d^{-1}, respectively. Assuming that the mean affinities are representative of their groups, affinities predict that N-replete cyanobacteria are more efficient at acquiring Fe than chlorophytes and should dominate when Fe is low but greater than their Fe_T.
3. A second study evaluated the competitive abilities of a pico-cyanobacterium and a third chlorophyte in dual species, serial dilution culture. The pico-cyanobacterium was dominant at 50 nmol L^{-1} total Fe (which limited both taxa) and 500 nmol L^{-1} total Fe. At 0.5 nmol L^{-1} total Fe, a stressful concentration below Fe_T during most of the incubation, growth rates and cell densities were extremely low but neither had washed out after several months.
4. These results show that Monod kinetics can successfully predict competition outcomes in laboratory settings at low Fe. While important, Monod kinetics are only one mechanism governing competition between cyanobacteria and eukaryotes in natural systems. Observed deviations from Monod predictions can be partially explained with known mechanisms.

KEYWORDS

nutrient thresholds, low iron, Monod growth affinity, dual species competition, cyanobacteria, eukaryotic algae

1. INTRODUCTION

Iron (Fe) is an important micronutrient for cellular growth and proliferation of phytoplankton populations. It is a co-factor in approximately 30% of oxidoreductase enzymes with known structure (Andreini et al., 2008) and is integral to many pathways including respiration, photosynthesis and nitrogen (N) fixation (Shi et al., 2007; Waldron & Robinson, 2009). Despite being abundant in the Earth's crust, free (uncomplexed) dissolved Fe is typically in low supply in the euphotic zone of aquatic environments due to the low solubility of the dominant oxidized ferric form (free Fe^{+3}), with the majority of total dissolved Fe^{+3} chelated to dissolved organic compounds (Molot & Dillon, 2003; McKay et al., 2005; Neal et al., 2008; Sorichetti et al., 2014; Du et al., 2019). Despite relatively small amounts of Fe needed by phytoplankton compared to N and phosphorus (P), Fe limitation of phytoplankton has been observed in several eutrophic aquatic systems with elevated demand for nutrients (Wurtsbaugh & Horne, 1983; Evans & Prepas, 1997; Twiss et al., 2000; Downs et al., 2008; Romero, et al., 2013; Schmidt, 2018). Fe limitation has also been observed in ocean waters (Brand, 1991; Martin et al., 1994 Nature 371; Maldonado & Price, 1999).

Cyanobacteria could be more susceptible to Fe limitation than eukaryotic algal growth because of their higher Fe requirements, especially when dependent on N fixation which requires Fe as a cofactor (Molot et al., 2014; Dixon & Kahn, 2004). Yet, their higher cellular demand has not deterred dominance of large-bodied (filamentous and colonial) cyanobacteria in many eutrophic systems (Downing et al., 2001; Paerl & Huisman, 2009) or the prevalence of pico-cyanobacteria across a trophic range (Vörös et al., 1998; Bell & Kalff, 2001; Callieri & Stockner, 2002; Callieri et al., 2007), suggesting that cyanobacterial capacity for acquiring Fe may be greater than eukaryotic phytoplankton.

The ability to acquire a nutrient can be represented with membrane transport and growth kinetic parameters. Fe transport can be described using the Michaelis-Menten model (Caperon & Meyer, 1972),

$$v = v_{max}\left(\frac{C_{Fe} - Fe_T}{K_{Fe} + C_{Fe} - Fe_T}\right)$$

where v is the Fe transport rate, v_{max} is the maximum transport rate, C_{Fe} is the concentration of Fe, Fe_T is the threshold concentration of Fe, and K_{Fe} is the half-saturation constant which is the concentration of Fe when the v is half the value of v_{max}. The initial slope as C_{Fe} approaches Fe_T, called the transport affinity, is given by $v_{max}/(K_{Fe} - Fe_T)$ (Molot & Brown, 1986) and is an indicator of transport efficiency at low C_{Fe}. K_{Fe} cannot be used by itself to infer relative competitive efficiency compared to other species except when their v_{max} values are similar.

By analogy, the relationship between growth rate and Fe concentration under pseudo-steady state conditions is described by the Monod equation,

$$\mu = \mu_{max}\left(\frac{C_{Fe} - Fe_T}{K_{Fe} + C_{Fe} - Fe_T}\right)$$

where μ is the growth rate and μ_{max} is the maximum growth rate at high C_{Fe} (Monod, 1950; Goldman et al., 1974; Kilham, 1975; Jiang et al., 2019). Similarly, the growth affinity as C_{Fe} approaches Fe_T is given by $\mu_{max}/(K_{Fe} - Fe_T)$ (Healey, 1980).

Both of these models are simplified in the sense that they do not incorporate steps that may be rate limiting such as Fe reduction prior to uptake (Shaked et al., 2005; Sutak et al., 2012) nor do they explicitly include the effects of Fe debt (degree to which Fe is needed), temperature (Goldman & Carpenter, 1974), light (Sunda & Huntsman, 2015), and binding strength of different organic ligands in media (Jones et al., 2015).

Nutrient kinetics can be empirically useful for predicting the outcome of species competition (Taylor & Williams, 1975; Titman, 1976; Kilham & Hecky, 1988; Sommer, 1993), however, there is little information comparing phytoplankton threshold concentrations and affinities for Fe. Transport parameters have been determined for several freshwater cyanobacteria species and a marine diatom (Sunda et al., 1991; Fujii et al., 2011; Rudolf et al., 2015; Fu et al., 2019) and growth parameters have been determined for several eukaryotic marine species (Sunda et al., 1991; Sunda & Huntsman, 1995; Jabre & Bertrand, 2020) under varying conditions. Published Monod equation parameters are summarized in Table 1.

This paper combines two studies. The first addresses the Monod parameter data gap by determining μ_{max}, K_{Fe} and Fe_T for three common, temperate freshwater large-bodied cyanobacteria and two chlorophyte species which were used to estimate their growth affinities, taken to represent their relative competitive abilities at low Fe. The second study explores the competitive abilities of a pico-cyanobacterium and a chlorophyte under three Fe concentrations in dual species serial dilution cultures with a view to understanding whether Monod kinetics can predict competition outcomes in a laboratory setting. We then discuss how other mechanisms may constrain Monod predictions in natural systems.

2. METHODS

2.1 Monod parameterization study

Cultures of the cyanobacteria *Dolichospermum (formerly Anabaena) flos-aquae* (CPCC 67), *Aphanizomenon skuja* (Lake 227 isolate) and *Microcystis aeruginosa* (PCC 7005), and the chlorophytes *Chlamydomonas reinhardtii* (CPCC 243) and *Chlorella vulgaris* (CPCC 90) were grown at 20 °C in either BG11 for the cyanobacteria, or Bolds basal medium (BBM) for the chlorophytes in deionized water with an equivalent amount of Co as $CoSO_4$ instead of $Co(NO_3)_2$ (Rippka et al., 1979; Stein et al., 1973). *Dolichospermum* and *Aphanizomenon* were also grown in $BG11_0$ without $NaNO_3$ and are referred to below as "N-deplete" to distinguish those cultures from those with $NaNO_3$ (N-replete). Cultures were grown in 50 mL Falcon tubes with a working volume of 30 mL on orbital platform shakers with a 12:12 hr light/dark cycle at 100 µmol m^{-2} s^{-1}.

All species were grown in 1 nmol L^{-1} Fe as $FeCl_3$ for three transfers before 1 mL of exponentially growing cells was transferred into a Falcon tube containing the appropriate media. Each Monod curve was based on 10 Fe concentrations varying from 0 to 1000 nmol L^{-1}. All containers were soaked in 10% trace metal grade HCl over 48 hours and then in deionized Milli-Q water for another 24 hours. Only acid-washed clear pipette tips were used throughout this experiment. All media, glassware, and disposable supplies were UV irradiated in a laminar flow hood for 15 minutes.

Absorbance at 750 nm (A_{750}) was used as an indicator of cell number. At 750 nm, interference from photosynthetic pigments is minimal and can be used as a consistent proxy for cell number (Chioccioli et al., 2014). Cell numbers were counted with a hemocytometer for comparison to A_{750}.

The *R* package *growthcurver* (version 0.3.0) was used to estimate the growth rate, μ, of each culture (Sprouffske & Wagner, 2016). This package finds the best fit of a given dataset to the logistic growth equation:

$$N_t = \frac{K}{1 + \left(\frac{K - N_0}{N_0}\right) e^{-\mu t}}$$

where N_t is the A_{750} at a given time, K is the carrying capacity, N_0 is the initial A_{750}, t is time and μ is the growth rate. The initial dissolved Fe concentration and associated μ were then fitted to the modified Monod growth equation using the *nls* function in *R* with bootstrapping (number of iterations = 10,000) (McClanahan & Humphries, 2012) used to solve for μ_{max}, Fe_T and K_{Fe}. Initial slopes were then calculated as $\mu_{max}/(K_{Fe} - Fe_T)$. Confidence intervals (CI) for each parameter were estimated from the bootstrapped iterations. One way analysis of variance (ANOVA) and post hoc Tukey's HSD test compared means based on bootstrapped values.

2.2 Competition study

The freshwater pico-cyanobacterium *Synechococcus leopoliensis* (CPCC 102) and the chlorophyte *Pseudokirchneriella subcapitata* (CPCC 37; formerly *Selenastrum capricornutum*) were grown separately and together in semi-continuous (serial dilution) cultures in a range of Fe concentrations. A pico-cyanobacterium was chosen because of the lower likelihood of inhibitory allelopathic interactions.

Cultures were grown in Bold 3N medium modified from BBM without vitamins or soil extract in deionized water (Table S1). Fe was varied while all other nutrient concentrations were held constant. Total P was 172 μmol L^{-1} and the total N to total P (TN:TP) molar ratio was 51.4. The media was adjusted to pH 7.0 prior to microwave-sterilization (Keller et al., 1988) and cooled to room temperature before inoculation.

Experiments were conducted using 50 ml of culture in 125 ml borosilicate Erlenmeyer flasks with gauze-covered cotton batting bungs. All flasks were mixed 24 hours per day at 75 rpm on rotary platform shaker tables. Continuous illumination was provided by fluorescent bulbs with light intensity ranging from 47.4 to 53.8 µmol m^{-2} s^{-1}, depending on each flask's position on the shaker table. To minimize the effect of different light levels, flasks were moved to different locations on the shaker table three times per week. Temperature varied between experiments, ranging from 22 to 26 °C.

To assay for the presence of allelopathy, both species were grown in single species batch cultures, first in defined media at 50 nmol L^{-1} Fe and then in the sterilized, spent filtrate from the other species (0.2 µm membrane filter) amended with modified Bold 3N nutrients with 50 nmol L^{-1} Fe and 172 µmol L^{-1} P. Abundance was measured as absorbance at 680 nm (*P. subcapitata*) and 672 nm (*S. leopoliensis*).

Three serial dilution competition experiments were conducted at 0.5 nmol L^{-1}, 50 nmol L^{-1} and 500 nmol L^{-1} total Fe. Each competition experiment included single species cultures and dual species cultures run simultaneously. Serial dilution was used rather than batch cultures because periodic provision of fresh media maintains growth of the less competitive species for a longer time, allowing for inspection of long-term dynamics. Before the start of each experiment, a starter culture of each species was grown at 0.5 nmol L^{-1} Fe. When the starter cultures reached mid-exponential growth phase, approximately 2 ml was transferred with a sterile disposable pipette to each of the experimental flasks containing 50 ml of sterile medium. The volume of the inoculum was adjusted in each experiment to ensure that the same concentration of algae (measured as average absorbance or optical density, OD, from 680 to 685 nm) initiated the culture in each flask. Each of the higher Fe concentrations (50 and 500 nmol L^{-1} Fe) had four replicate flasks while three replicates were used at 0.5 nmol L^{-1} Fe.

Whenever growth monitoring indicated that the cultures were in late-exponential to early-stationary phase, 25 mL of each were transferred into a new flask containing 25 ml of sterile medium (i.e., a 50 % dilution rate). The frequency of dilution varied depending on the Fe concentration of each experiment with greater dilution frequency at higher Fe. Population density was measured in samples immediately before and after dilution and between dilutions.

Due to large errors associated with direct microscopy counts of *S. leopoliensis* which tended to form colonies of varying size (Callieri, 2010) making accurate counting of cells difficult, three optical measurements were used as proxies of biomass concentrations in single and dual species cultures: mean absorbance between 680-685 nm (optical density, OD), and fluorescence at two different excitation/emission wavelengths: 585/660 nm (sensitive to cyanobacterial phycocyanin and therefore a good measure of *S. leopoliensis*) and 470/685 nm (sensitive to chlorophyll with a greater intensity in eukaryotes, and therefore a good measure of *P. subcapitata*). Fluorescence was corrected for inner filter quenching with $F_{corr} = F_{obs}\ 10^{(Odex + Odem)/2}$ where F_{corr} is the corrected fluorescence, F_{obs} is the observed fluorescence, and OD_{ex} and OD_{em} are the absorbances at excitation and emission wavelengths, respectively (Lakowicz, 1999). The relationships between OD and fluorescence in single species cultures were inspected to confirm their species specificity, and then compared to fluorescence in dual species cultures to determine if either species had become dominant. The outcome of each competition experiment was verified semi-quantitatively at the end of each experiment by microscopy inspection of 18 haemocytometer grids per replicate flask and recording the presence or absence of each species in each grid.

Equilibrium free Fe^{+3} concentrations in Bold 3N medium without phytoplankton were calculated using Visual MINTEQ 3.1 (Gustafsson, 2013) assuming pH 7.0 and a solution temperature of 24 °C. Input components are listed in Table S2. It was assumed that all metal inputs were in their fully oxidized states.

3. RESULTS

3.1 Monod parameterization study

Absorbance at 750 nm (A_{750}) was strongly correlated with cell density with $R^2 \geq 0.99$ for all species except *Aphanizomenon skuja* which was slightly lower with $R^2 = 0.96$. This indicates that absorbance is a valid proxy of population size. Phytoplankton growth curves were sigmoidal (Figure S1). Boxplots for each species are shown in Figure S2.

The Monod parameters (Fe_T, K_{Fe} and μ_{max}) of each species were estimated from μ and their corresponding initial dissolved Fe concentration (Figure 1). Low root mean squared errors (RMSE) between 0.007 and 0.019 indicate that each Monod curve was a good fit to the μ estimated from the logistic equation.

The mean Monod parameter (Fe_T, K_{Fe} and μ_{max}) values for each species and their 95% confidence intervals from the bootstrapped values are presented in Table 2. Parameter estimates for the N fixers are shown for two growing conditions – with added N (N-replete) and without added N (N-deplete). Parameter ranges were 0.021 – 1.204 nmol L^{-1} for Fe_T, 0.222 – 1.461 nmol L^{-1} for K_{Fe} and 0.181 – 0.209 d^{-1} for μ_{max}. Tukey's HSD post hoc test showed that most of the species' mean bootstrapped parameters were significantly different from each other with two exceptions: Fe_T for *Aphanizomenon skuja* and *Chlorella vulgaris*, and K_{Fe} for *Chlamydomonas reinhardtii* and *Chlorella vulgaris* were not significantly different from each other.

The Fe_T reported in this study (0.021 – 1.204 nmol L^{-1}) are slightly lower than those reported for eukaryotic marine algae which ranged from 1.2-10 nmol L^{-1} (Table 1). The latter are the lowest concentrations with observable growth rates rather than the highest concentration with a zero growth rate as defined in the Monod growth equation which may account for their higher values. Based on the pooled data, it is likely that Monod Fe_T values for most phytoplankton are below 5 nmol L^{-1} (measured as total dissolved Fe), values too low to be measured with the colorimetric ferrozine method (Verschoor and Molot, 2013).

Results were pooled into four groups: all cyanobacteria with and without N (n = 5), N-replete cyanobacteria (n = 3), N-deplete cyanobacteria (i.e., when N-fixing; n = 2), and chlorophytes (n = 2) (Table 3). Mean values for N-replete cyanobacteria, N-deplete cyanobacteria and chlorophytes for Fe_T were 0.076, 0.736 and 0.245 nmol L^{-1}; for K_{Fe} were 0.341, 1.093 and 0.745 L nmol L^{-1}; and for μ_{max} were 0.195, 0.194 and 0.198 d^{-1}. Tukey's HSD post hoc test showed that the group means for Fe_T, μ_{max} and K_{Fe} were significantly different from each other. N-replete cyanobacteria had a lower mean Fe_T than the chlorophytes while N-fixing cyanobacteria had a higher mean Fe_T. The latter would not necessarily be a competitive disadvantage to N-fixers in a low Fe system that was N-limited.

The affinity or relative growth ability at low concentrations of Fe, was calculated as the initial slope of the Monod curve, $\mu_{max}/(K_{Fe} - Fe_T)$ for each species and group (Table 4). A higher affinity indicates a competitive advantage for a species at similar low Fe concentration. *Chlorella vulgaris*, the eukaryotic algae, had the lowest affinity at 0.332 L $nmol^{-1}$ d^{-1}, while N-replete *Dolichospermum flos-aquae* and *Microcystis aeruginosa* had the highest affinities (> 1 L $nmol^{-1}$ d^{-1}). Mean affinities for all cyanobacteria, N-replete cyanobacteria, N-deplete cyanobacteria and chlorophytes were 0.822, 0.971, 0.597 and 0.412 L d^{-1} $nmol^{-1}$, respectively. Mean chlorophyte affinities were not significantly different from the three cyanobacteria groups (all, N-replete, N-deplete) at the 5% level because there was only one degree of freedom. Nevertheless, both chlorophyte affinities were smaller than the five cyanobacteria affinities and if this pattern is representative of their taxonomic groups, then Monod kinetic parameters predict that cyanobacteria are more efficient at acquiring Fe than chlorophytes when Fe is low but greater than their Fe_T.

3.2 Competition study

Final yields of *Pseudokirchneriella subcapitata* and *Synechococcus leopoliensis* in single species cultures were clearly lower at 50 nmol L^{-1} (molar P/Fe ratio of 3440) compared to final yields at 0.5 µmol L^{-1} and 750 nmol L^{-1} (Figure 2). Hence, we concluded that 50 nmol L^{-1} Fe was growth limiting.

Spent filtrate from each species stimulated the growth rate and final yield of the other species at 50 nmol L^{-1} Fe (Figure 3). Hence, allelopathic growth inhibition during competition experiments likely did not occur. Addition of nutrients to spent filtrate may have been responsible for growth stimulation.

At 50 and 500 nmol L^{-1} Fe, optical density vs fluorescence relationships in single species culture at 470/685 nm excitation/emission for *P. subcapitata* and 585/660 nm excitation/emission for *S. leopoliensis* were linear with high R^2 over wide ranges (Figures 4 and 5). Therefore, these two emission/excitation combinations were used to identify whether *P. subcapitata* or *S. leopoliensis* was dominant in dual species cultures at the two higher Fe concentrations. In contrast, at 0.5 nmol L^{-1} Fe there was poor separation of the two OD-fluorescence curves at 470/685 nm and no

separation at 585/660 nm (Figure 6). Hence, fluorescence was not suitable for distinguishing the dominant species at this low Fe concentration.

At the highest Fe concentration in the serial dilution experiments, 500 nmol L^{-1} Fe, half of the culture media was replaced with fresh media every 3 to 4 days. Optical densities (Figure 7a) were similar in single and dual species cultures indicating similar biomass yields. All cultures reached quasi steady state after two dilution cycles and remained stable until the experiment was terminated after 10 dilution cycles, seven weeks after inoculation. The experimental conditions should be considered 'quasi' steady state rather than steady state because temporal oscillations were induced by serial dilution at regular intervals. Fluorescence in the dual species cultures were similar to *S. leopoliensis* and not *P. subcapitata* fluorescence in the single species cultures after the first two dilution cycles (Figure 7b and 7c) suggesting that *S. leopoliensis* was dominant thereafter. *P. subcapitata* fluorescence values in Figure 7b and 7c were about an order of magnitude smaller than fluorescence in single species *S. leopoliensis*. A plot of 585/660 nm fluorescence in *S. leopoliensis* single species culture vs dual species culture was close to the 1:1 line with a slope of 0.75 (Figure 7d), suggesting that *P. subcapitata* was rare in this dual species experiment and that *S. leopoliensis* was dominant after several dilution cycles. Visual inspection of dual species cultures by microscopy at the end of the experiment confirmed that *S. leopoliensis* was clearly dominant: one *P. subcapitata* cell was found in 18 haemacytometer grids in each of two replicate flasks and no cells were found in the other two replicates.

At 50 nmol L^{-1} Fe culture media was replaced every six or seven days for approximately three months (Figure 8). Cultures became stable after four dilution cycles with similar biomass yields in all three cultures (Figure 8a). Fluorescence values in the dual species cultures were similar to *S. leopoliensis* fluorescence in single species cultures after two dilution cycles and not *P. subcapitata* fluorescence in single species cultures (Figure 8b and 8c). A plot of 585/660 nm fluorescence in *S. leopoliensis* single species culture vs dual species culture was close to the 1:1 line with a slope of 0.91 (Figure 8d), indicating that *S. leopoliensis* was dominant after several dilution cycles. *P. subcapitata* fluorescence values in Figure 8b and 8c were about an order of magnitude smaller than fluorescence in *S. leopoliensis* single species cultures and dual species cultures, suggesting that *P. subcapitata* was very rare in this dual species culture. Visual inspection of dual species cultures by microscopy at the end of the experiment (11 dilution

cycles) revealed only *S. leopoliensis* and *P. subcapitata* was not observed in any of the replicates.

Growth was quite slow at the lowest iron concentration, 0.5 nmol L^{-1} Fe, consequently, the 5.5-month duration of this experiment was much longer than in the higher Fe experiments. Half of the media was replaced every 4 weeks. These Fe-stressed cultures did not exhibit the regular periodicity observed at higher Fe concentrations (Figure 9a-c). There was poor separation of *S. leopoliensis* and *P. subcapitata* fluorescence curves at both emission/excitation wavelength pairs. Separation at 585/660 nm was marginally better than at 475/685 nm but not enough to have confidence that *S. leopoliensis* was more abundant (Figures 9d and 9e). Hence, a clear statement of coexistence based on fluorescence was not possible. However, visual inspection of dual species cultures by microscopy after 5 dilution cycles (after 5.5 months) revealed that both species were observed in all 18 grids in all replicates indicating some level of co-existence. Severe Fe stress appears to have lowered cellular content of phycocyanin: the mean ratio ($\pm$ one standard deviation) of fluorescence at 585/660 nm to optical density was only 16 $\pm$ 23 compared to 105 $\pm$ 26 at 50 nmol L^{-1} Fe and 59 $\pm$ 4 at 500 nmol L^{-1} Fe.

Modeled free Fe^{+3} equilibrium concentrations in modified Bold 3N media before inoculation were 7.95 x 10^{-12}, 7.87 x 10^{-10} and 7.1 x 10^{-9} pmol L^{-1} at 0.5, 50 and 500 nmol L^{-1} total dissolved Fe, respectively. These are many orders of magnitude smaller than the proxy free ferric Fe_T for marine eukaryotes in Table 1 which were in the 2 - 10 pmol L^{-1} range, perhaps because the latter include $Fe(OH)_2^+$ and $Fe(OH)_4^-$. The ratio of free Fe^{3+} to total Fe was extremely small, ranging from 1.3 x 10^{-14} to 1.6 x 10^{-14} indicating that only a tiny proportion of dissolved Fe^{+3} was available for uptake at any one time. Extracellular free Fe^{3+} concentrations were probably declined after inoculation of *P. subcapitata* and *S. leopoliensis* due to Fe uptake. Biologically reduced free Fe^{2+} concentrations were probably orders of magnitude less than the free Fe^{3+} concentrations because of rapid re-oxidation and transport.

4. DISCUSSION

4.1 Monod parameters predict cyanobacteria dominance under some Fe conditions

Assuming that the mean Fe_T and growth affinities for cyanobacteria and chlorophytes when N is non-limiting are representative of these freshwater groups, the results suggest that Fe concentrations between 0.076 and 0.245 nmol L^{-1} favour dominance by N-replete cyanobacteria because concentrations in this range are above the mean threshold for N-replete cyanobacteria but below the mean chlorophyte threshold of 0.245 nmol L^{-1} (Table 3). Low Fe concentrations greater than 0.245 nmol L^{-1} will also favour N-replete cyanobacteria because cyanobacteria have higher affinities at low Fe (0.822 vs 0.412 L $nmol^{-1}$ day^{-1}, Table 4). Thus, these Monod parameters predict that cyanobacteria are generally favoured to dominate when members of the phytoplankton community are Fe limited barring other factors (discussed below).

Severe N depletion lead to the N fixers having higher Fe_T and lower affinities (Tables 2-4). Perhaps the fixers utilize a less efficient Fe transport system when Fe is not severely limiting, one that is less costly to maintain. However, this would not put them at a competitive disadvantage when N is limiting.

Two cautionary notes regarding extrapolating these parameters to other settings. First, Monod and transport parameters may vary to some extent among strains adapted to differing environments. Strains of a marine diatom and pico-cyanobacteria adapted to low Fe environments have been observed to invest in more efficient Fe acquisition apparatus and biochemistries adapted to low Fe than strains in regions with higher Fe availability (Brand, 1991; Sunda et al, 1991; Sunda and Huntsman, 1995; Gilbert et al., 2022). Second, the growth affinity and Fe_T values in this study are based on synthetic culture media with one chelator, EDTA. Each chelator has a unique binding affinity for free (uncomplexed) Fe^{+3} which is the main chemical species transported across the cell membrane by eukaryotic algae. Chelators also exhibit different Fe^{+2} oxidation rates thus potentially affecting cyanobacteria transport rates (Molot et al., 2010; Lis et al., 2015). Hence, the absolute values of these Monod parameters must be treated with caution when applied to other synthetic and natural systems. Nevertheless, relative values would probably still apply in a system dominated by one chelator.

4.2 Competition study: Fe affinities and resource competition theory support Monod predictions

In the serial dilution experiments, the pico-cyanobacterium *Synechococcus leopoliensis* dominated the cultures at the two higher Fe concentrations. Assuming that *S. leopoliensis* has a similar growth affinity to other cyanobacteria such as *Do flos-aquae*, *A. skuja* and *M. aeruginosa*, and that the chlorophyte *Pseudokirchneriella subcapitata* has a similar growth affinity to other chlorophytes such as *Chlorella vulgaris* and *Chlamydomonas reinhardtii*, then the success of *S. leopoliensis* at 50 nmol L^{-1} Fe is predicted by the Monod results. This assumption is supported by another study that showed that *D. flos-aquae* and *Synechococcus* Nagelii have P transport affinities similar to each other, and both are larger than the P transport affinities of the eukaryotic algae *Navicula pelliculosa*, *P. kirchneriella* Printz and *Scenedesmus quadricauda* (Molot & Brown, 1986). However, predictions of competition outcomes based on P affinities haves not been tested.

Dominance by *S. leopoliensis* at 500 nmol L^{-1} Fe could have been due to denial of Fe to *P. kirchneriella* or by limitation by another nutrient, e.g., P, that favours *S. leopoliensis*. In either case, dominance by one species when both are limited by the same nutrient is predicted by resource competition theory (Taylor & Williams, 1975; Titman, 1976; Sommer, 1993).

Severe Fe-limitation at 0.5 nmol L^{-1} near or below their Fe_T severely stressed both species allowing neither a competitive advantage. Fe was too far below the hypothetical Fe 'sweet spot' to create dual nutrient limitation, i.e., limitation of *S. leopoliensis* by Fe and limitation of *P. subcapitata* by a different nutrient allowing co-existence. This 'sweet spot', possibly as low as 1 or 2 nmol L^{-1}, must be high enough to avoid severe Fe stress in both species while low enough to limit *S. leopoliensis* but not *P. subcapitata*. The results of the 0.5 nmol L^{-1} experiment also suggest that in principle, no species will dominate if all are severely nutrient deprived, i.e., all suffer from at least one nutrient at a concentration below the threshold.

4.3 Implications

The value of this study and that of Molot & Brown (1986) lies in the knowledge that large-bodied and pico-cyanobacteria appear to be superior competitors to eukaryotic algae for Fe and P at low concentrations. While nutrient limitation is clearly a major factor structuring phytoplankton communities, these Monod predictions cannot explain certain observations in

natural systems which suggests that Monod predictions are not the only mechanism operating in natural systems. While nutrient transport and growth kinetic considerations are important, at times they need to be reconciled with in situ observations by considering other mechanisms.

For example, (1) pico-cyanobacteria and eukaryotic algae often co-exist in oligotrophic systems that are apparently P-limited (Vörös et al., 1998; Bell & Kalff, 2001; Callieri & Stockner, 2002; Callieri et al., 2007). Resource partitioning theory predicts that co-existence is not possible unless each of the dominant species is limited by a different nutrient (Taylor and Williams, 1975; Titman, 1976; Sommer, 1993) yet Fe growth kinetic from this study and P transport kinetic data (Molot et al., 1986) indicate that cyanobacteria should dominate when Fe and P are limiting. Perhaps pico-cyanobacteria and eukaryotes co-exist because pico-cyanobacteria are limited by something other than P in oligotrophic waters. Genetically modified pico-cyanobacteria bioreporters and nutrient bioassays have indicated Fe deficiency at different times and places in Lake Superior and Lake Erie (Twiss et al., 2000; McKay et al., 2005; Porta et al., 2005; Twiss et al., 2005) but it is unclear how widespread Fe limitation of pico-cyanobacteria is. Another possibility is that intensive grazing pressure on pico-cyanobacteria restricts their abundance and recycles nutrients, allowing room for eukaryotic algae to grow and co-exist or even become dominant (Cavender-Bares et al., 1999; Mann & Chisholm, 2000; Stockner et al., 2000).

(2) We also note that large-bodied cyanobacteria typically dominate eutrophic systems during warm periods regardless of the type of limiting nutrient (Fe, P and N) except in high nitrate systems, even though these high nitrate systems are probably limited by P or a metal (Beutel et al., 2016; Molot et al., 2021, 2022). Evidence suggests that onset of anaerobic sediments at accessible depths to buoyancy-regulating large-bodied cyanobacteria promotes cyanobacteria blooms across a trophic range in warm waters (Molot et al., 2014, 2021, 2022). The link between low sediment redox and blooms is likely increased supply of a redox-sensitive metal and not P or N since blooms also occur in N-rich, P-limited oligotrophic waters without internal P loading (albeit not as dense) (Carey et al., 2008; Winter et al., 2011; Verschoor et al., 2017; Reinl et al., 2021). In addition, cyanobacteria have a greater affinity for P and so should be favoured at low P. Internally loaded Fe^{+2} is the most plausible candidate for this shift towards dominance of large-bodied cyanobacteria (Molot et al., 2014, 2021) although internal loading rates of manganese (as Mn^{+2}) are also high. Perhaps large-bodied cyanobacteria, unlike pico-

cyanobacteria, use their ability to regulate their buoyancy to position themselves near these sediment sources (Camacho et al., 1996; Camacho, Vicente & Miracle, 2000; Gervais et al., 2003; Head, Jones & Bailey-Watts, 1999) allowing them to acquire the Fe^{+2} needed to support a bloom. In this scenario, eukaryotic algae are excluded, even those that are motile, by their lower affinities for P in P-limited systems, perhaps aided by allelopathic inhibition, as large-bodied cyanobacteria become Fe-replete. Of course, in N-limited eutrophic systems, N fixation by cyanobacteria excludes eukaryotic algae. Fe-limitation of cyanobacteria in eutrophic systems has been reported but these may be cases where blooms outstrip Fe supply rates in later stages of development as they increase in size (Wurtsbaugh & Horne, 1983; Downs et al., 2008; Evans & Prepas, 1997).

(3) Finally, we elaborate here on the question of why pico-cyanobacteria and not large-bodied species fill the cyanobacteria niche in oligotrophic waters. Pico-cyanobacteria are apparently favoured over large-bodied cyanobacteria at very low nutrient concentrations because of their higher cell surface area/volume ratio (Sunda & Huntsman, 1995; Smith & Kalff, 1983). However, the proportion of pico-cyanobacteria contribution phytoplankton biomass declines with increasing P (Bell and Kalff, 2001; Callieri and Stockner, 2002). If all cyanobacteria have similar transport rates per unit cell surface area, it follows that nutrient supply rates to a volumetric intracellular region are larger in smaller cells which would lead to less limitation within a cell. This is not a new idea. However, since internal nutrient loading from anaerobic sediments is generally absent in oligotrophic lakes except in certain morphological circumstances (Verschoor et al., 2017), large-bodied cyanobacteria cannot use their ability to regulate their buoyancy to acquire anaerobic sources and thus must compete with pico-cyanobacteria for open water sources where they are at a disadvantage. This disadvantage disappears as productivity and associated anaerobic conditions increase.

5. SUMMARY

In this study we quantified the Monod Fe parameters for several common freshwater phytoplankton species including three bloom-forming cyanobacteria and two chlorophytes and used their initial slopes at low Fe as measures of their relative competitiveness. The prediction that lower Fe_T and higher affinity in N-replete cyanobacteria favours them over eukaryotic algae

in low Fe culture was successfully tested in dual species, serial dilution culture using different cyanobacteria and chlorophyte species. Hence, nutrient kinetic models such as the Monod model can provide a basis for understanding community composition, at least at the coarse taxonomic level of cyanobacteria vs chlorophyte applied in this study. While important, nutrient kinetics are only one mechanism governing competition between cyanobacteria and eukaryotic algae in natural systems and work is needed to reconcile and couple them with other mechanisms.

SUPPORTING INFORMATION

Additional supporting information may be found online in the Supporting Information section.

AUTHOR CONTRIBUTIONS

All authors contributed to the study conception and design. Experiment preparation, sample collection and analyses, and data analyses were performed by Purnank Shah and Shelley McCabe. The first draft of the manuscript was written by Purnank Shah and Lewis Molot and all authors edited and commented on all versions of the manuscript. All authors read and approved the final manuscript.

ACKNOWLEDGEMENTS

We would like to thank S.B. Watson and A. Zastepa at Environment Canada and Climate Change's Canada Centre for Inland Waters (CCIW) for isolating a strain of *Aphanizomenon skuja* from Lake 227 at the Experimental Lakes Area (IISD-ELA). We are grateful to G. Braun and the Centre for Cold Regions and Water Science at Wilfrid Laurier University for access to and training in the use of the analytical equipment used in this study. This study was funded by Natural Sciences and Engineering Research Council of Canada (NSERC) Strategic Partnership Grant for Projects, STPGP 494497-2016 and NSERC Discovery Grant to L. Molot.

CONFLICT OF INTEREST

The authors declare that they have no conflicts of interest.

DATA AVAILABILITY STATEMENT

The datasets generated and/or analysed during the current study are available from the corresponding author upon reasonable request.

ORCID

Jason J. Venkiteswaran https://orcid.org/0000- 0002-6574-7071
Lewis A. Molot https://orcid.org/0000-0003-4059-7369
Sherry L. Schiff https://orcid.org/0000- 0002-7704-7304

REFERENCES

Andreini, C., Bertini, I., Cavallaro, G., Holliday, G. L., & Thornton, J. M. (2008). Metal ions in biological catalysis: from enzyme databases to general principles. *Journal of Biological Inorganic Chemistry*, *13*(8), 1205–1218. https://doi.org/10.1007/s00775-008-0404-5.

Beutel, M. W., Duvil, R., Cubas, F. J., Matthews, DA, Wilhelm, FM, Grizzard, T. J., Austin, D., Horne, A. J. & Gebremariam, S. (2016). A review of managed nitrate addition to enhance surface water quality. *Critical Reviews in Environmental Science Technology*, 46, 673-700.

Bell, T. & Kalff, J. (2001). The contribution of picophytoplankton in marine and freshwater systems of different trophic status and depth. *Limnology and Oceanography*, 46, 1243-1248.

Brand, L. (1991). Minimum iron requirements of marine phytoplankton and the implications for the biogeochemical control of new production. *Limnology and Oceanography*, 36, 1756-1771.

Callieri, C. (2010). Single cells and microcolonies of freshwater picocyanobacterial: a common ecology. *Journal of Limnology*, 69, 257-277, DOI: 10.3274/JL10-69-2-08

497 Callieri, C. & Stockner, J. G. (2002). Freshwater autotrophic picoplankton: a review.
498 *Journal of Limnology*, 61, 1-14.

499 Callieri, C., Modenutti, B., Queimalinos, C., Bertoni, R., & Balseiro, E. (2007). Production
500 and biomass of picophytoplankton and larger autotrophs in Andean ultraoligotrophic lakes:
501 differences in light harvesting efficiency in deep layers. *Aquatic Ecology*, 41, 511-523.

502 Camacho, A., Garcia-Pichel, F., Vicente, E., & Castenholz, R.W. (1996). Adaptation to
503 sulfide and to the underwater light field in three cyanobacterial isolates from Lake Arcas
504 (Spain). *FEMS Microbiology Ecology*, 21, 293-301.

505 Camacho, A., Vicente, E., & Miracle, M. (2000). Ecology of a deep-living *Oscillatoria*
506 (=*Planktothrix*) population in the sulphide-rich waters of a Spanish karstic lake, *Archiv für*
507 *Hydrobiologie*, 148, 333-355.

508 Caperon, J. & Meyer, J. (1972). Nitrogen-limited growth of marine phytoplankton - II.
509 Uptake kinetics and their role in nutrient limited growth of phytoplankton. *Deep Sea*
510 *Research*, 19, 619-632.

511 Carey, C. C., Weathers, K. C., & Cottingham, K. L. (2008). *Gloeotrichia echinulata* blooms
512 in an oligotrophic lake: helpful insights from eutrophic lakes. *Journal of Plankton Research*,
513 30, 893-904.

514 Cavender-Bares, K. K., Mann, E. L., Chisholm, S. W., Ondrusek, M. E., & Bidigare, R. R.
515 (1999). Differential response of equatorial Pacific phytoplankton to iron fertilization.
516 *Limnology and Oceanography*, 44, 237-246.

517 Chioccioli, M., Hankamer, B., & Ross, I. L. (2014). Flow cytometry pulse width data
518 enables rapid and sensitive estimation of biomass dry weight in the microalgae
519 Chlamydomonas reinhardtii and Chlorella vulgaris. *PLoS ONE*, *9*(5), 1–12.
520 https://doi.org/10.1371/journal.pone.0097269.

Dixon, R., & Kahn, D. (2004). Genetic regulation of biological nitrogen fixation. *Nature Reviews Microbiology*, 2, 621-631.

Downing, J. A., Watson, S. B., & McCauley, E. (2001). Predicting Cyanobacteria dominance in lakes. *Canadian Journal of Fisheries and Aquatic Sciences, 58*(10), 1905–1908. https://doi.org/10.1139/cjfas-58-10-1905.

Downs, T. M., Schallenberg, M., & Burns, C. W. (2008). Responses of lake phytoplankton to micronutrient enrichment: a study in two New Zealand Lakes and an analysis of published data. *Aquatic Sciences*, 70, 347-360.

Du, X. L., Creed, I. F., Sorichetti, R. J. & Trick, C. G. (2019). Cyanobacteria biomass in shallow eutrophic lakes is linked to the presence of iron-binding ligands. *Canadian Journal of Fisheries and Aquatic Sciences*, 76, 1728–1739. dx.doi.org/10.1139/cjfas-2018-0261.

Evans, J. C. & Prepas, E. E. (1997). Relative importance of iron and molybdenum in high phosphorus saline lakes. *Limnology and Oceanography*, 42, 461-472.

Fu, Q.-L., Fujii, M., Natsuike, M., & Waite, T. D. (2019). Iron uptake by bloom-forming freshwater cyanobacterium Microcystis aeruginosa in natural and effluent waters. *Environmental Pollution*, 247, 392-400.

Fujii, M., Dang, T. C., Bligh, M. W., Rose A. L. & Waite, T. D. (2014) Effect of natural organic matter on iron uptake by the freshwater cyanobacterium *Microcystis aeruginosa*. *Environmental Science and Technology*, 48, 365-374.

Gervais, F., Siedel, U., Heilmann, B., Weithoff, G., Heisig-Gunkel, G., & Nicklisch, A. (2003). Small-scale vertical distribution of phytoplankton, nutrients and sulphide below the oxycline of a mesotrophic lake. *Journal of Plankton Research*, 25, 273-278.

Gilbert, N. E., LeCleir, G. R., Strzepek, R. F., Ellwood, M. J., Twining, B. S., Roux, S., Pennacchio, C., Boyd, P. W., & Wilhelm, S. W. (2022). Bioavailable iron titrations reveal oceanic *Synechococcus* ecotypes optimized for different iron availabilities. *ISME Commun.* 2,54. https://doi.org/10.1038/s43705-022-00132-5.

Goldman, J. C., Oswald, W. J. & Jenkins, D. (1974). The kinetics of inorganic carbon limited algal growth. *Journal of the Water Pollution Control Federation,* 46. 554-574.

Goldman, J. C. & Carpenter, E. J. (1974). A kinetic approach to the effect of temperature on algal growth. *Limnology and Oceanography*, 19, 756-766.

Gustafsson, J. P. (2013). Visual MINTEQ version 3.1, beta. KTH Royal Institute of Technology: Sustainable Development, Environmental Science and Engineering. Stockholm, Sweden. http://vminteq.lwr.kth.se/download/, viewed on June 17, 2014.

Head, R. M., Jones, R. I., & Bailey-Watts, A. E. (1999). Vertical movements by planktonic cyanobacteria and the translocation of phosphorus: implications for lake restoration. *Aquatic Conservation: Marine Freshwater Ecosystems*, 9(1), 111–120.

Healey, F. P. (1980). Slope of the Monod equation as an indicator of advantage in nutrient competition. *Microbial Ecology*, *5*(4), 281–286. https://doi.org/10.1007/BF02020335.

Jabre, L. & Bertrand, E. M. (2020). Interactive effects of iron and temperature on the growth of *Fragilariopsis cylindrus. Limnology and Oceanography Letters,* 5, 363-370.

Jiang, M., Zhou, Y., Cao, X., Ji, X., Zhang, W., Huang, W., Zhang, J., & Zheng, Z. (2019). The concentration thresholds establishment of nitrogen and phosphorus considering the effects of extracellular substrate-to-biomass ratio on cyanobacterial growth kinetics. *Science of The Total Environment*, 662, 307–312. https://doi.org/10.1016/j.scitotenv.2019.01.184.

Jones, A. M., Griffin, P. J. & Waite, T. D. (2015). Ferrous iron oxidation by molecular oxygen under acidic conditions: The effect of citrate, EDTA and fulvic acid. *Geochimica et Cosmochimica Acta*, 160, 117-131. doi.org/10.1016/j.gca.2015.03.026.

569 Keller, M. D., Bellows, W. K. & Guillard, R. R. L. (1988). Microwave treatment for
570 sterilization of phytoplankton culture media. *Journal of Experimental Marine Biology and*
571 *Ecology*, 117, 279-283. doi.org/10.1016/0022-0981(88)90063-9.

572 Kilham, S. S. (1975). Kinetics of silicon-limited growth in the freshwater diatom
573 *Asterionella formosa*. *Journal of Phycology*, 11, 396–399. https://doi.org/10.1111/j.1529-
574 8817.1975.tb02802.

575 Kilham, P. & Hecky, R. E. (1988). Comparative ecology of marine and freshwater
576 phytoplankton. *Limnology and Oceanography*, 33, 776-795.

577 Lakowicz, J. R. (1999). Principles of fluorescence spectroscopy. 2nd edition, Kluwer
578 Academic/Plenum Publishers, New York, 698 p.

579 Maldonado M. T. & Price N. M. (1999). Utilization of iron bound to strong organic ligands
580 by plankton communities in the subarctic Pacific Ocean, *Deep-Sea Research Part II:*
581 *Topical Studies in Oceanography*, 46, 2447-2473, doi:10.1016/S0967-0645(99)00071-5.

582 Mann, E. L. & Chisholm, S. W. (2000). Iron limits the cell division rate of *Prochlorococcus*
583 in the eastern equatorial Pacific. *Limnology and Oceanography*, 45, 1067-1076.

584 Martin, J. H., Coale, K. H., Johnson, K. S., Fitzwater, S. E., Gordon, R. M., Tanner, S. J.,
585 Hunter, C. N., Elrod, V. A., Nowicki, J. L., Coley. T. L., & Barber, R. T. (1994). Testing
586 the iron hypothesis in ecosystems of the equatorial Pacific Ocean. *Nature*, 371, 123-129.

587 McClanahan, T. R., & Humphries, A. T. (2012). Differential and slow life-history responses
588 of fishes to coral reef closures. *Marine Ecology Progress Series*, *469*, 121–131.
589 https://doi.org/10.3354/meps10009.

590 McKay, R. M. L., Porta, D., Bullerjahn, G. S., Al-Rshaidat, M. M. D., Klimowicz, J. A.,
591 Sterner, R. W., Smutka, T. M., Brown, E. T., & Sherrell, R. M. (2005). Bioavailable iron in
592 oligotrophic Lake Superior assessed using biological reporters. *Journal of Plankton*
593 *Research*, 27(10), 1033–1044. https://doi.org/10.1093/plankt/fbi070.

Molot, L. A., & Brown, E. J. (1986). Method for determining the temporal response of microbial phosphate transport affinity. *Applied and Environmental Microbiology*, 51(3), 524–531. https://doi.org/10.1128/AEM.51.3.524-531.1986.

Molot, L. A., and Dillon, P. J. (2003) Variation in iron, aluminum and dissolved organic carbon mass transfer coefficients in lakes. *Water Research*, 37(8), 1759-1768. https://doi.org/10.1016/S0043-1354(02)00424-4.

Molot, L. A., Li, G., Findlay, D. L. & Watson, S. B. (2010). Iron-mediated suppression of bloom-forming cyanobacteria by oxine in a eutrophic lake, *Freshwater Biology*, 55, 1102-1117. doi:10.1111/j.1365-2427.2009.02384.x.

Molot, L. A., Schiff, S. L., Venkiteswaran, J. J., Baulch, H. M., Higgins, S. N., Zastepa, A., Verschoor, M. J., & Walters, D. (2021). Low sediment redox promotes cyanobacteria blooms across a trophic range: implications for management. *Lake and Reservoir Management*, 37, 120–142. https://doi.org/10.1080/10402381.2020.1854400.

Molot, L. A., Watson, S. B., Creed, I. F., Trick, C. G., McCabe, S. K., Verschoor, M. J., Sorichetti, R. J., Powe, C., Venkiteswaran, J. J., & Schiff, S. L. (2014). A novel model for cyanobacteria bloom formation: the critical role of anoxia and ferrous iron. *Freshwater Biology*, *59*(6), 1323–1340. https://doi.org/10.1111/fwb.12334.

Molot, L. A., Depew, D. C., Zastepa, A., Arhonditsis, G. B., Watson, S. B., & Verschoor, M. J. (2022). Long-term and seasonal nitrate trends illustrate potential prevention of large cyanobacterial biomass by sediment oxidation in Hamilton Harbour, Lake Ontario. *Journal of Great Lakes Research*, 48: 971-984, doi.org/10.1016/j.jglr.2022.05.014.

Monod, J. (1950). Technique, theory and applications of continuous culture. *Annales de l'Institut Pasteur*, *79*, 390–410. https://www.cabdirect.org/cabdirect/abstract/19512703495.

Neal, C., Lofts, S., Evans, C. D., Reynolds, B., Tipping, E. & Neal, M. (2008). Increasing iron concentrations in UK upland waters. 2008. *Aquatic Geochemistry*, 14, 263–288. DOI 10.1007/s10498-008-9036-1.

620 Paerl, H. W. & Huisman, J. (2009). Climate change: a catalyst for global expansion of
621 harmful cyanobacterial blooms. *Environmental Microbiology Reports*, 1(1), 27-37.
622 https://doi.org/10.1111/j.1758-2229.2008.00004.x.

623 Porta, D., Bullerjahn G. S., Twiss, M. R., Wilhelm, S. W., Poorvin, L., & McKay, R. M. L.
624 (2005). Determination of bioavailable Fe in Lake Erie using a luminescent cyanobacterial
625 bioreporter. *Journal of Great Lakes Research*, 31(Suppl 2), 180-194.

626 Reinl, K. L., Brookes, J. D., Carey, C. C., Harris, T. D., Ibelings, B. W., Morales-Williams,
627 A. M., De Senerpont Domis, L. N., Atkins, K. S., Isles, P. D., Mesman, J. & North, R. L.,
628 (2021). Cyanobacterial blooms in oligotrophic lakes: shifting the high-nutrient paradigm.
629 *Freshwater Biology*, 66, 1846-1859. DOI: 10.1111/fwb.13791.

630 Rippka, R., Deruelles, J., Waterbury, J. B., Herdman, M., & Stanier, R. Y. (1979). Generic
631 Assignments, Strain Histories and Properties of Pure Cultures of Cyanobacteria.
632 *Microbiology*, *111*, 1–61. https://doi.org/10.1099/00221287-111-1-1.

633 Romero, I. C., Klein, N. J., Sañudo-Wilhelmy, S. A., & Capone, D. G. (2013). Potential
634 trace metal co-limitation controls on N_2 fixation and NO_3 uptake in lakes with varying
635 trophic status. *Frontiers in Microbiology*, 4, 1-12. doi: 10.3389/fmicb.2013.00054.

636 Rudolf, M., Kranzler, C., Lis, H., Margulis, K., Stevanovic, M., Keren, N., & Schleiff, E.
637 (2015). Multiple modes of iron uptake by the filamentous, siderophore-producing
638 cyanobacterium, *Anabaena* sp. PCC 7120. *Molecular Microbiology*, 97(3), 577–588.
639 doi.org/10.1111/mmi.13049.

640 Schmidt, B. M. (2018). Nitrogen fixation in lakes: Response to micronutrients and
641 exploration of a novel method of measurement. MS thesis, Kent State University, Ohio.
642 http://rave.ohiolink.edu/etdc/view?acc_num=kent1524172083482442.

643 Shaked, Y., Kustka, A. B. & Morel, F. M. M. (2005). A general kinetic model for iron
644 acquisition by eukaryotic phytoplankton. *Limnology and Oceanography*, 50, 872-882.

Shi, T., Sun, Y., & Falkowski, P. G. (2007). Effects of iron limitation on the expression of metabolic genes in the marine cyanobacterium *Trichodesmium erythraeum* IMS101. *Environmental Microbiology*, 9, 2945–2956. https://doi.org/10.1111/j.1462-2920.2007.01406.x.

Smith, R. & Kalff, J. (1983). Competition for Phosphorus among co-occurring freshwater phytoplankton, *Limnology and Oceanography*, 28, 448-464.

Sommer, U. (1993) Phytoplankton competition in Plußsee - a field test of the resource-ratio hypothesis. *Limnology and Oceanography*, 38, 838-845.

Sorichetti, R. J., Creed, I. F., & Trick, C. G. (2014). Evidence for iron-regulated cyanobacterial predominance in oligotrophic lakes. *Freshwater Biology*, 59, 679-691. doi:10.1111/fwb.12295.

Sprouffske, K., & Wagner, A. (2016). Growthcurver: an R package for obtaining interpretable metrics from microbial growth curves. *BMC Bioinformatics*, *17*(1), 172. https://doi.org/10.1186/s12859-016-1016-7.

Stein, J. R., Hellebust, J. A., & Craigie, J. S. (1973). *Handbook of phycological methods: culture methods and growth measurements*. Cambridge University Press.

Sunda W.G., Swift D.G. & Huntsman S.A. (1991). Low iron requirement for growth in oceanic phytoplankton. *Nature,* 351, 55-57.

Sunda, W. G. & Huntsman, S. A. (1995). Iron uptake and growth limitation in oceanic and coastal phytoplankton. *Marine Chemistry*, 50, 189-206.

Sunda, W. G., & Huntsman, S. A. (2015). High iron requirement for growth, photosynthesis, and low-light acclimation in the coastal cyanobacterium *Synechococcus bacillaris*. *Frontiers in Microbiology*, *6*, 1-13. https://doi.org/10.3389/fmicb.2015.00561.

Sutak, R., Botebol, H., Blaiseau, P.-L., Léger, T., Bouget, F.-Y., Camadro, J.-M., & Emmanuel Lesuisse. (2012). A Comparative study of iron uptake mechanisms in marine microalgae: iron

670 binding at the cell surface is a critical step. *Plant Physiology*, 160, 2271-2284.
671 www.plantphysiol.org/cgi/doi/10.1104/pp.112.204156.

672 Twiss, M. R., Auclair, J.-C., & Charlton, M. N. (2000) An investigation into iron-stimulated
673 phytoplankton productivity in epipelagic Lake Erie during thermal stratification using trace
674 metal clean techniques, *Canadian Journal of Fisheries and Aquatic Sciences*, 57, 86-95,
675 doi:10.1139/cjfas-57-1-86.

676 Twiss, M. R., Gouvêa, S.P., Bourbonniere, R.A., McKay, R.M.L. & Wilhelm, S.W. (2005).
677 Field investigations of trace metal effects on Lake Erie phytoplankton productivity. *Journal*
678 *of Great Lakes Research*, 31(Suppl 2), 168-179.

679 Verschoor, M. J., & Molot, L. A. (2013). A comparison of three colorimetric methods of
680 ferrous and total reactive iron measurement in freshwaters. *Limnology Oceanography*
681 *Methods*, 11, 113-125.

682 Verschoor, M. J., Powe, C. R., McQuay, E., Schiff, S. L., Venkiteswaran, J. J., Li, J., &
683 Molot, L. A. (2017). Internal iron loading and warm temperatures are preconditions for
684 cyanobacterial dominance in embayments along Georgian Bay, Great Lakes. *Canadian*
685 *Journal of Fisheries and Aquatic Sciences*, 74(9), 1439–1453. https://doi.org/10.1139/cjfas-
686 2016-0377.

687 Vörös, L., Callieri, C., Balogh, K., & Bertoni, R. (1998). Freshwater picocyanobacteria
688 along a trophic gradient and light quality range. *Hydrobiologia*, 370, 117–125.

689 Waldron, K. J. & Robinson, N. J. (2009). How do bacterial cells ensure that metalloproteins
690 get the correct metal? *Nature Reviews*, 6, 25-35.

691 Winter, J. G., DeSellas, A. M., Fletcher, R., Heintsch, L., Morley, A., Nakamoto, L., &
692 Utsumi, K. (2011). Algal blooms in Ontario, Canada: Increases in reports since 1994. *Lake*
693 *and Reservoir Management*, 27(2), 107–114.
694 https://doi.org/10.1080/07438141.2011.557765.

Wurtsbaugh, W. A., & Horne, A. J. (1983). Iron in eutrophic Clear Lake, California: Its Importance for algal nitrogen fixation and growth. *Canadian Journal of Fisheries and Aquatic Sciences*, 40, 1419 - 1429.

TABLE 1 Summary of published Fe Monod equation parameters for marine eukaryotic algae. Thresholds are referred to here as 'proxy' because they are the lowest concentrations with observable growth rates rather than the highest concentration with a zero growth rate as defined in the Monod equation. Inorganic Fe includes Fe^{+3}, $Fe(OH)_2^+$ and $Fe(OH)_4^-$.

Species	μ_{max} (d^{-1})	K_{Fe}	Fe_T proxy	Reference
Thalassiosira. oceanica	1.2			Sunda et al., 1991
T. oceanica	1.66		2 pmol L^{-1} as inorganic Fe	Sunda and Huntsman, 1995
T. pseudonana	1.75	100 pmol L^{-1} as inorganic Fe, 34 nmol L^{-1} as total Fe	<40 pmol L^{-1} as inorganic Fe, 10 nmol L^{-1} as total Fe	Sunda et al., 1991
T. pseudonana	1.80		10.3 pmol L^{-1} as inorganic Fe, 4.3 nmol L^{-1} as total Fe	Sunda and Huntsman, 1995
T. weissflogii	0.89		3 pmol L^{-1} as inorganic Fe, 1.2 nmol L^{-1} as total Fe	Sunda and Huntsman, 1995
Emiliana huxleyi	1.12		2 pmol L^{-1} as inorganic Fe, 1.2 nmol L^{-1} as total Fe	Sunda and Huntsman, 1995
Pelagomonas calceolata	1.05		3 pmol L^{-1} as inorganic Fe, 1.2 nmol L^{-1} as total Fe	Sunda and Huntsman, 1995
Prorocentrum minimum	0.58		3.3 pmol L^{-1} as inorganic Fe, 1.3 nmol L^{-1} as total Fe	Sunda and Huntsman, 1995
Fragilariopsis cylindrus at 6°C	0.34	23 pmol L^{-1} as free Fe	< 5 pmol L^{-1} as free Fe, 1.2 nmol L^{-1} as total Fe	Jabre and Bertrand, 2020

705 **TABLE 2** Mean Monod parameter values for individual species. The N fixers, *Dolichospermum*
706 *flos-aquae* and *Aphanizomenon skuja*, were grown with DIN (N-replete) and without DIN (N-
707 deplete). Letters indicate statistically different means at $p < 0.05$ using Tukey's HSD post hoc
708 test. Units are nmol L^{-1} for Fe_T and K_{Fe} and day^{-1} for μ_{max}.
709

Species	Tukey's HSD significance	Mean Value	95% CI		5% CI
	Fe_T				
Dolichospermum flos-aquae (N-replete)	f	0.021	0.022		0.021
Dolichospermum flos-aquae (N-deplete)	d	0.268	0.274		0.261
Aphanizomenon skuja (N-replete)	e	0.131	0.134		0.128
Aphanizomenon skuja (N-deplete)	a	1.204	1.235		1.174
Microcystis aeruginosa	b	0.663	0.680	0.647	
Chlamydomonas reinhardtii	c	0.347	0.356		0.339
Chlorella vulgaris	e	0.142	0.146		0.139
	K_{Fe}				
Dolichospermum flos-aquae (N-replete)	f	0.222	0.224		0.221
Dolichospermum flos-aquae (N-deplete)	d	0.726	0.731		0.721
Aphanizomenon skuja (N-replete)	e	0.46	0.463		0.457
Aphanizomenon skuja (N-deplete)	a	1.461	1.472		1.449
Microcystis aeruginosa	b	0.802	0.808	0.795	
Chlamydomonas reinhardtii	c	0.741	0.747		0.736
Chlorella vulgaris	c	0.748	0.755		0.742
	μ_{max}				
Dolichospermum flos-aquae (N-replete)	a	0.209	0.209		0.209
Dolichospermum flos-aquae (N-deplete)	e	0.185	0.186		0.185
Aphanizomenon skuja (N-replete)	g	0.181	0.181		0.181
Aphanizomenon skuja (N-deplete)	b	0.203	0.203		0.202
Microcystis aeruginosa	f	0.184	0.184	0.183	

Chlamydomonas reinhardtii	d	0.194	0.194		0.194
Chlorella vulgaris	c	0.201	0.202		0.201

710
711

TABLE 3 Mean Monod parameter values for phytoplankton groups. The N fixers, *Dolichospermum flos-aquae* and *Aphanizomenon skuja*, were grown with DIN (N-replete) and without DIN (N-deplete). 'All' includes the three cyanobacteria species in N-replete and N-deplete media (n = 5). Letters indicate statistically different means at $p < 0.05$ using Tukey's-HSD post hoc test. Units are nmol L^{-1} for Fe_T and K_{Fe} and day^{-1} for μ_{max}.

Group	Tukey's HSD significance	Mean Value	95% CI	5% CI
	Fe_T			
Cyanobacteria (all)	b	0.663	0.68	0.647
Cyanobacteria (N-replete fixers)	d	0.076	0.078	0.074
Cyanobacteria (N fixers, N-deplete)	a	0.736	0.753	0.719
Chlorophytes	c	0.245	0.25	0.24
	K_{Fe}			
Cyanobacteria (all)	b	0.802	0.808	0.795
Cyanobacteria (N-replete fixers)	d	0.341	0.343	0.339
Cyanobacteria (N-deplete fixers)	a	1.093	1.101	1.085
Chlorophytes	b	0.745	0.749	0.741
	μ_{max}			
Cyanobacteria (all)	d	0.184	0.184	0.183
Cyanobacteria (N-replete fixers)	b	0.195	0.195	0.195
Cyanobacteria (N-deplete fixers)	c	0.194	0.194	0.194
Chlorophytes	a	0.198	0.198	0.198

TABLE 4 Affinities (initial slope of the Monod growth curve) as defined by $\mu_{max}/(K_{Fe} - Fe_T)$ for individual species and groups at low concentrations of Fe. For individual species, ± is the propagated (combined) 95% confidence interval. For groups, $\pm$ is the standard deviation of the affinities for individual species. 'All' includes the three cyanobacteria species in N-replete and two in N-deplete media (n = 5). Units are L $nmol^{-1}$ day^{-1}.

Species	$\mu_{max}/(K_{Fe} - Fe_T)$
Dolichospermum flos-aquae (N-replete)	1.040 ± 0.008
Dolichospermum flos-aquae (N-deplete)	0.404 ± 0.007
Aphanizomenon skuja (N-replete)	0.550 ± 0.007
Aphanizomenon skuja (N-deplete)	0.790 ± 0.085
Microcystis aeruginosa	1.324 ± 0.172
Chlamydomonas reinhardtii	0.492 ± 0.012
Chlorella vulgaris	0.332 ± 0.004

Group	$\mu_{max}/(K_{Fe} - Fe_T)$
Cyanobacteria (all)	0.822 ± 0.371
Cyanobacteria (N-replete fixers)	0.971 ± 0.392
Cyanobacteria (N-deplete fixers)	0.597 ± 0.273
Chlorophytes (n = 2)	0.412 ± 0.114

FIGURE 1 Monod plots for each species. Horizontal dashed lines indicate μ_{max} and vertical dashed lines indicate Fe_T. '-N' indicates N-deplete. RMSE is between μ values estimated from logistic and Monod equations.

FIGURE 2 Optical density (mean 680-685 nm) of *P. subcapitata* and *S. leopoliensis* in batch culture at three Fe concentrations 50 nmol L^{-1} (green diamonds), 500 nmol L^{-1} (red squares) and 750 nmol L^{-1} (open triangles). Error bars are standard errors.

FIGURE 3 Optical density (mean 680-685 nm) of *P. subcapitata* and *S. leopoliensis* in single species batch cultures with and without spent filtrate from other species. Error bars are standard errors (n = 3). Red diamonds - control in Bold 3N with 50 nmol L^{-1} Fe; Green squares – spent filtered *P. subcapitata* filtrate amended with 50 nmol L^{-1} Fe and 172 μmol L^{-1} P; Open circles - spent filtered *S. leopoliensis* filtrate amended with 50 nmol L^{-1} Fe and 172 μmol L^{-1} P.

FIGURE 4 Optical density (mean 680-685 nm) vs fluorescence at two emission/excitation wavelength combinations in single species cultures at 500 nmol L^{-1} Fe. *P. subcapitata* (blue squares), *S. leopoliensis* (red circles).

FIGURE 5 Optical density (mean 680-685 nm) vs fluorescence at two emission/excitation wavelength combinations in single species cultures at 50 nmol L^{-1} Fe. *P. subcapitata* (blue squares), *S. leopoliensis* (red circles).

FIGURE 6 Optical density (mean 680-685 nm) vs fluorescence at two emission/excitation wavelength combinations in single species cultures at 0.5 nmol L^{-1} Fe. *P. subcapitata* (blue squares), *S. leopoliensis* (red circles).

FIGURE 7 Serial dilution experiments at 500 nmol L^{-1} Fe. A) Optical densities (mean 680-685 nm) vs time in single and dual species cultures, B) fluorescence at 470/685 nm vs time in single and dual species cultures, C) fluorescence at 585/660 nm vs time in single and dual cultures, and (D) fluorescence at 585/660 nm in single vs dual species cultures with 1:1 line. Key: blue squares - *P. subcapitata* in single species culture; red circles - *S. leopoliensis* in single species culture; green triangles in panels A to C - dual species culture.

FIGURE 8 Serial dilution experiments at 50 nmol L^{-1} Fe. A) Optical densities (mean 680-685 nm) vs time in single and dual species cultures, B) fluorescence at 470/685 nm vs time in single and dual species cultures, C) fluorescence at 585/660 nm vs time in single and dual species

cultures, and (D) fluorescence at 585/660 nm in single vs dual species cultures with 1:1 line. Key: blue squares - *P. subcapitata* in single species culture; red circles - *S. leopoliensis* in single species culture; green triangles in panels A to C - dual species culture.

FIGURE 9 Serial dilution experiments at 0.5 nmol L^{-1} Fe. A) Optical densities (mean 680-685 nm) vs time in single and dual species cultures, B) fluorescence at 475/685 nm vs time in single and dual species cultures, C) fluorescence at 585/660 nm vs time in single and dual species cultures, D) fluorescence at excitation/emission 475/685 nm in single vs dual species with 1:1 line, and E) fluorescence at excitation/emission 585/660 nm in single vs dual species with 1:1 line. Key: blue squares - *P. subcapitata* in single species culture; red circles - *S. leopoliensis* in single species culture; green triangles in panels A to C - dual species culture.

Figure 1

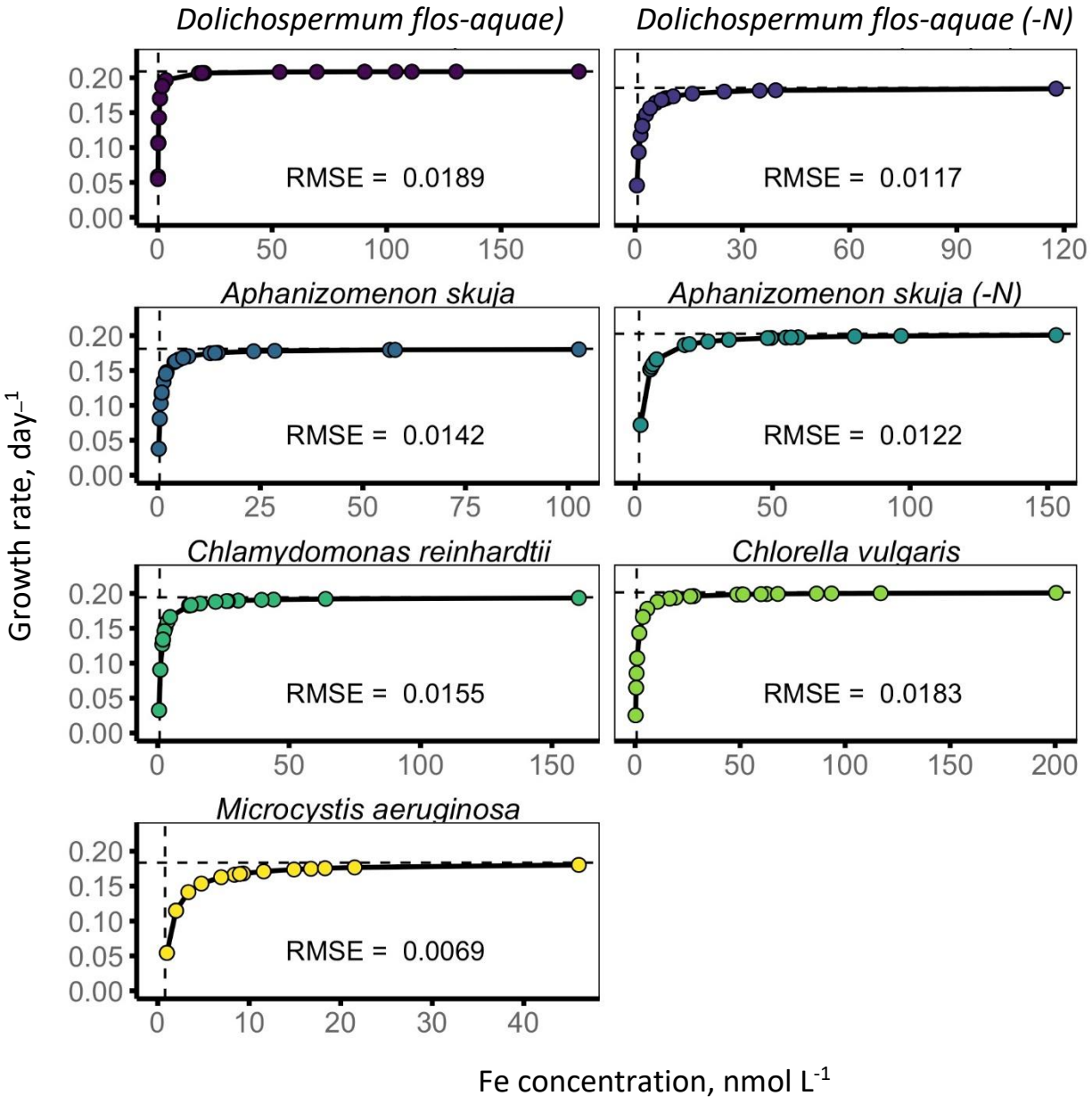
Dolichospermum flos-aquae)
Dolichospermum flos-aquae (-N)
RMSE = 0.0189
RMSE = 0.0117
Aphanizomenon skuja
Aphanizomenon skuja (-N)
RMSE = 0.0142
RMSE = 0.0122
Chlamydomonas reinhardtii
Chlorella vulgaris
RMSE = 0.0155
RMSE = 0.0183
Microcystis aeruginosa
RMSE = 0.0069
Growth rate, day-1
Fe concentration, nmol L-1

769

770 **Figure 2**

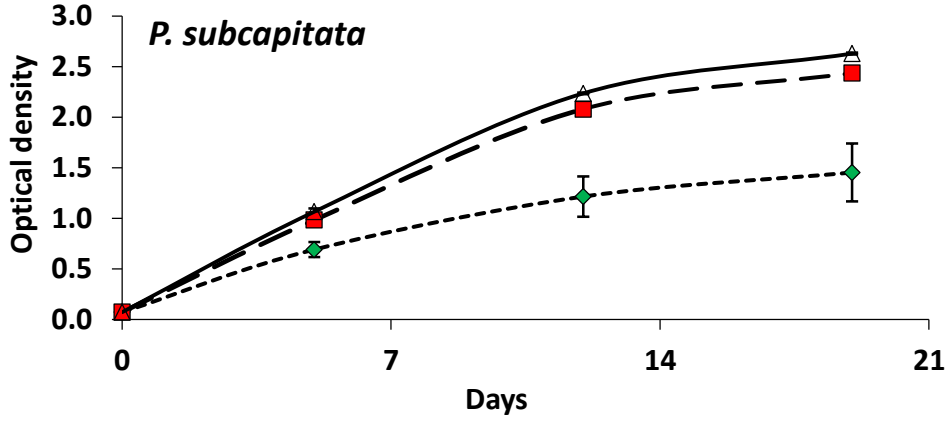

771

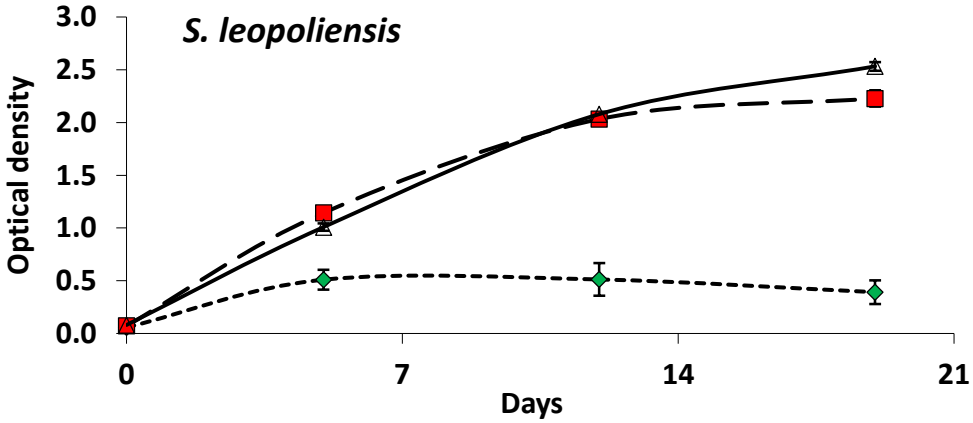

772

773 **Figure 3**

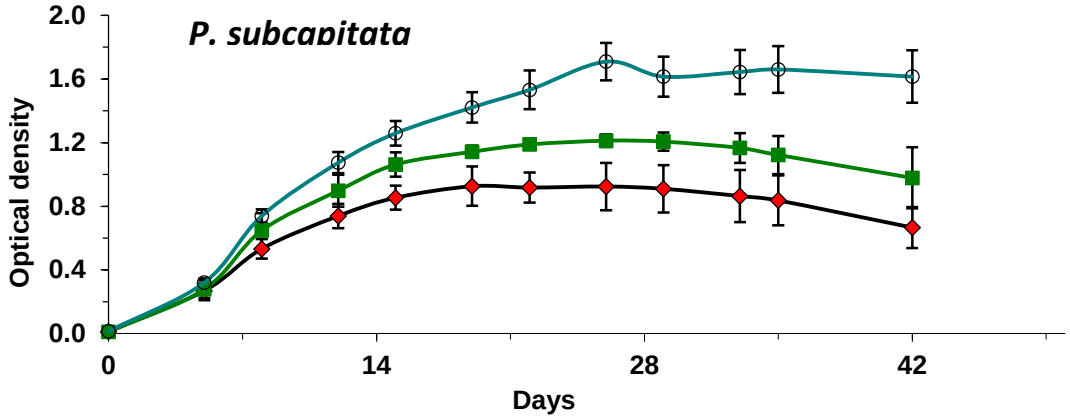

774

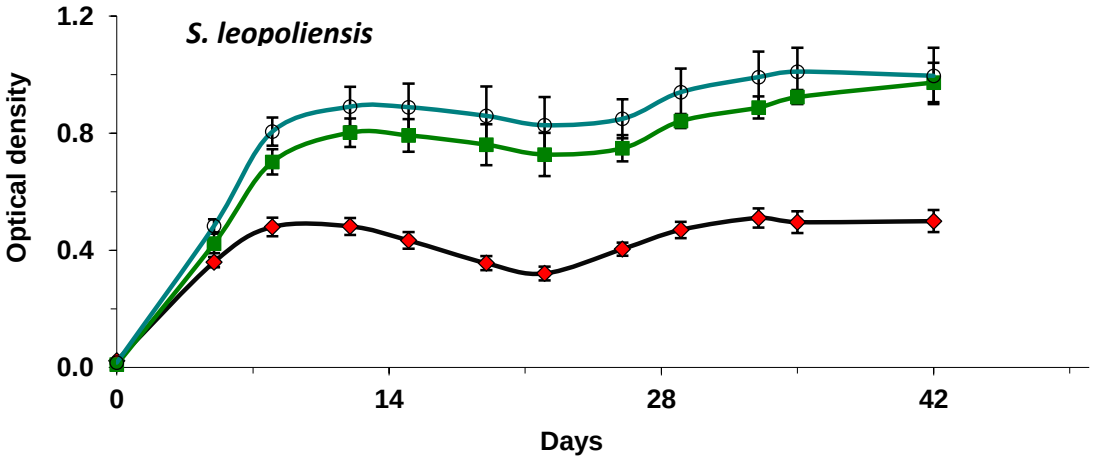

775

776 **Figure 4**

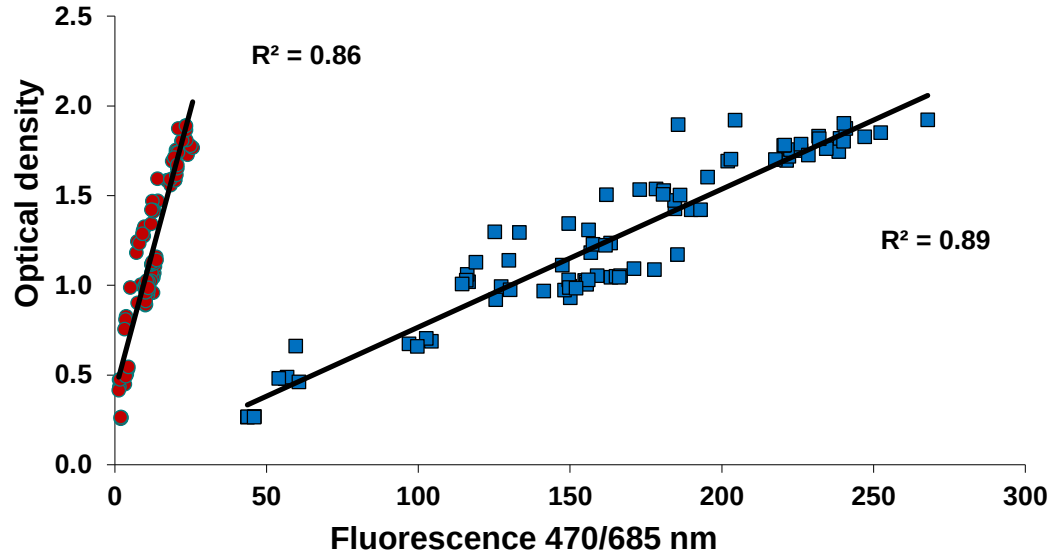

777

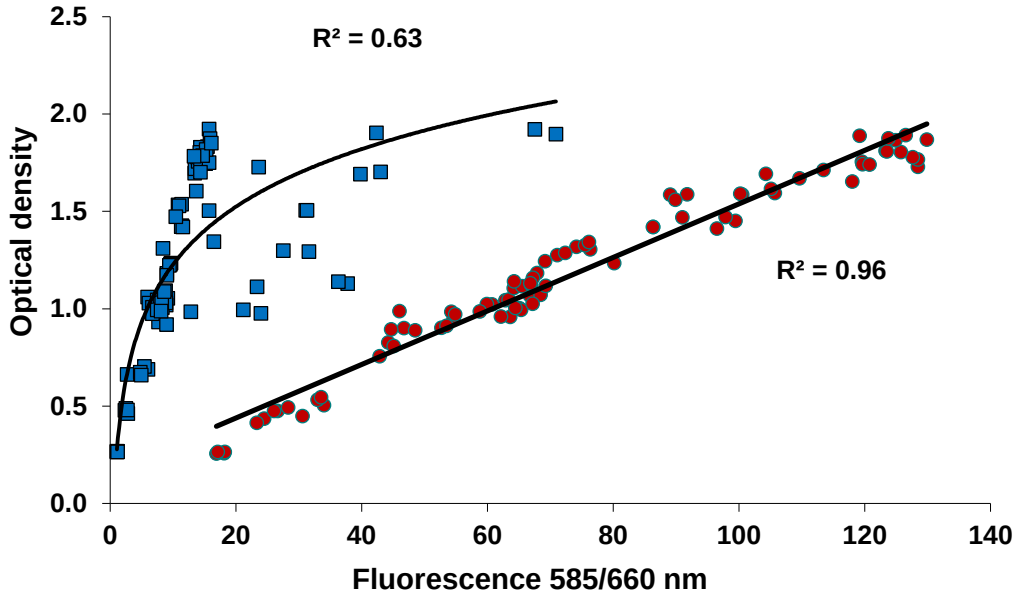

778

779

780 **Figure 5**

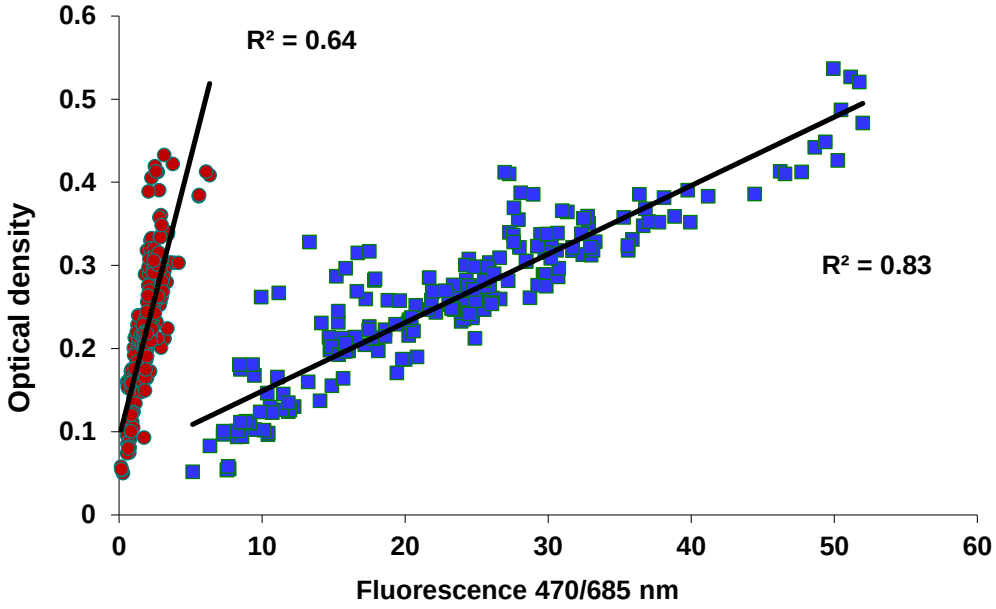

781

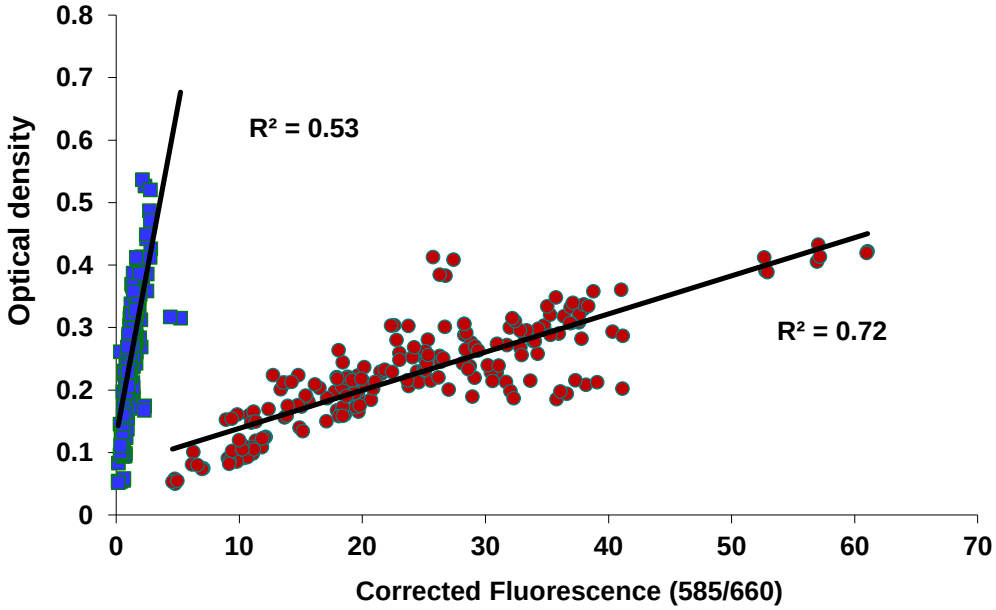

782

783 **Figure 6**

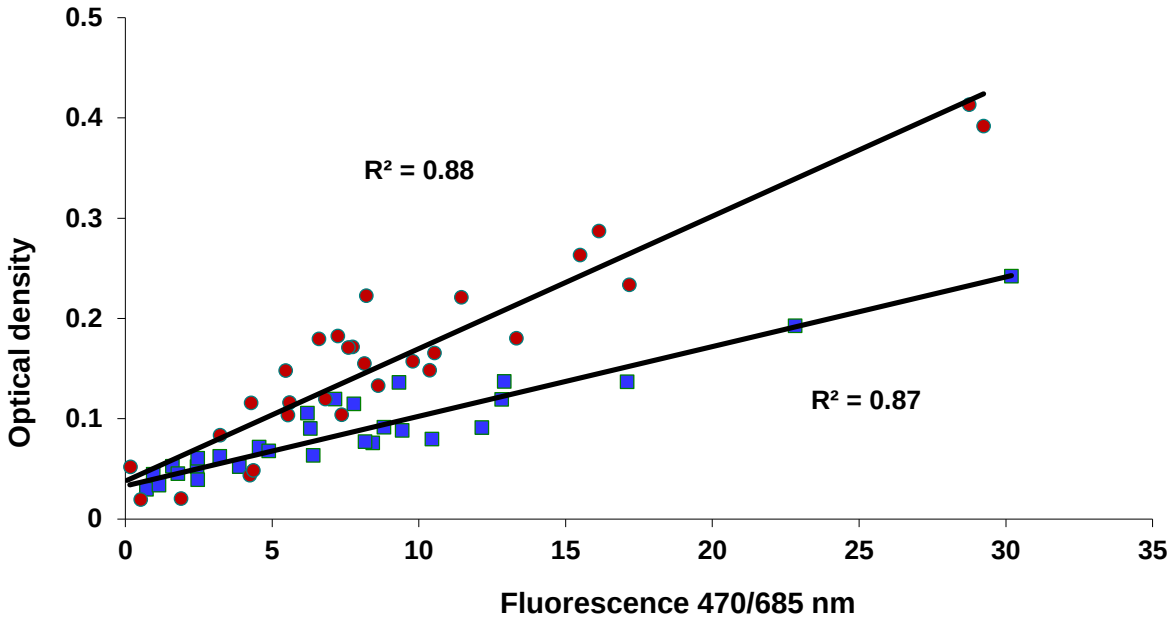

784

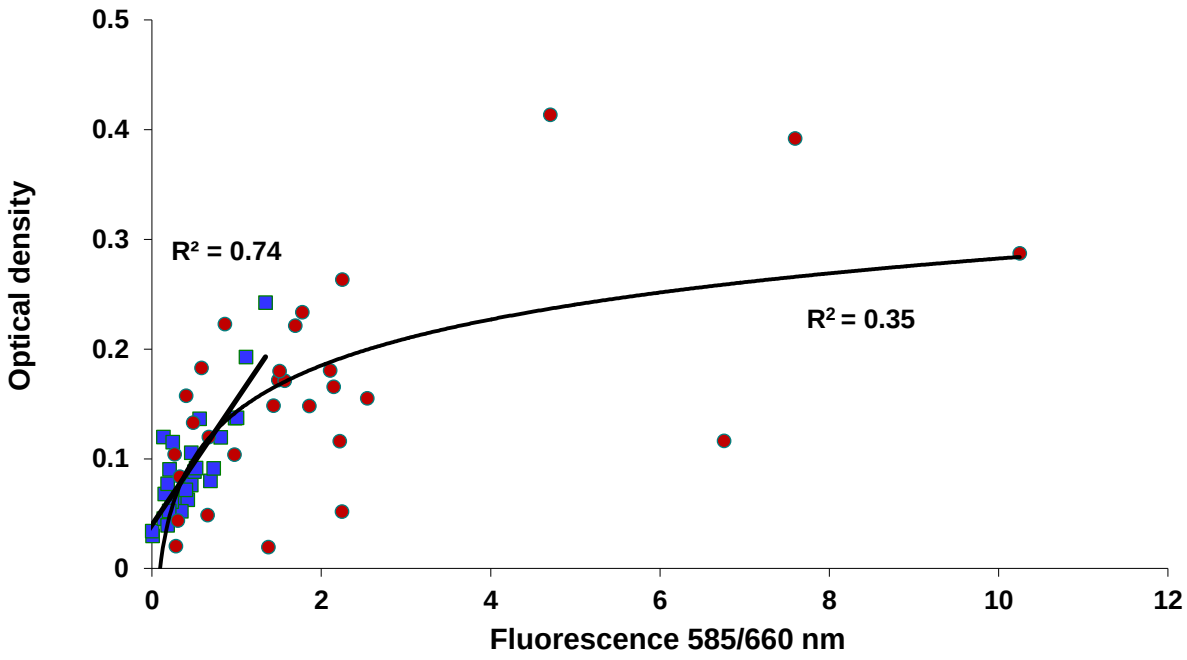

785

786

787 **Figure 7**

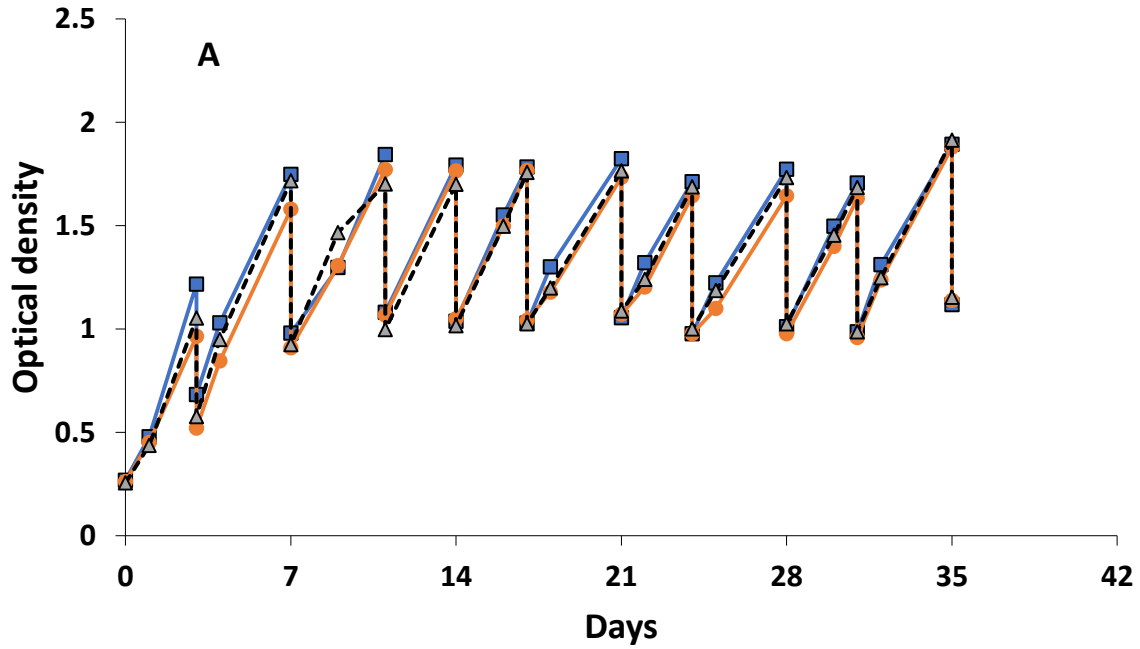

788

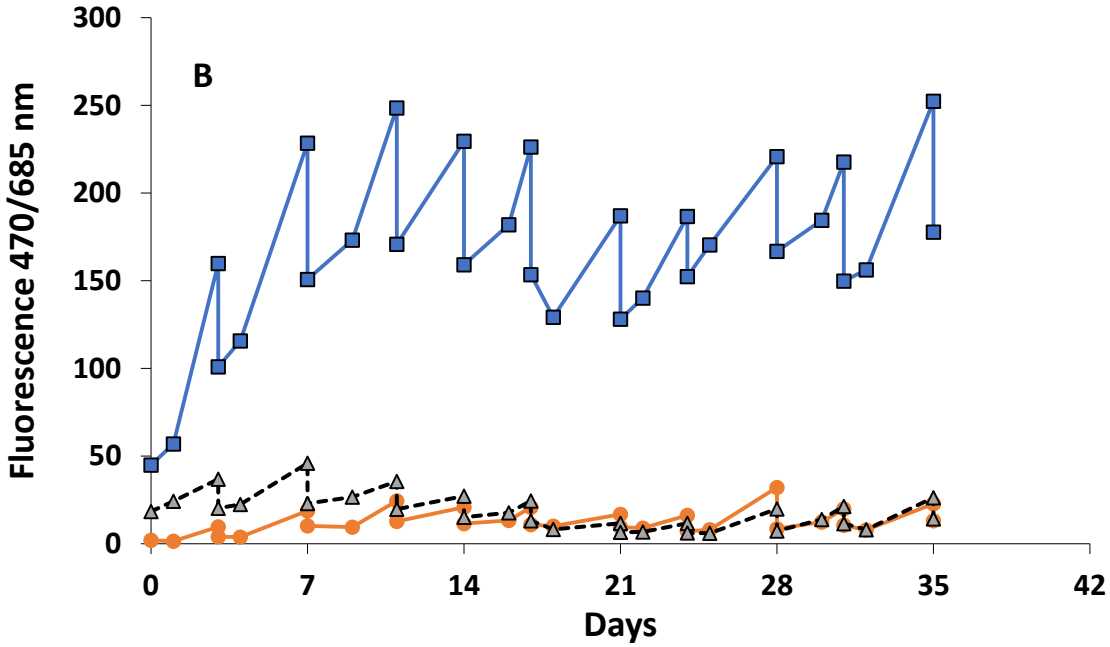

789

790

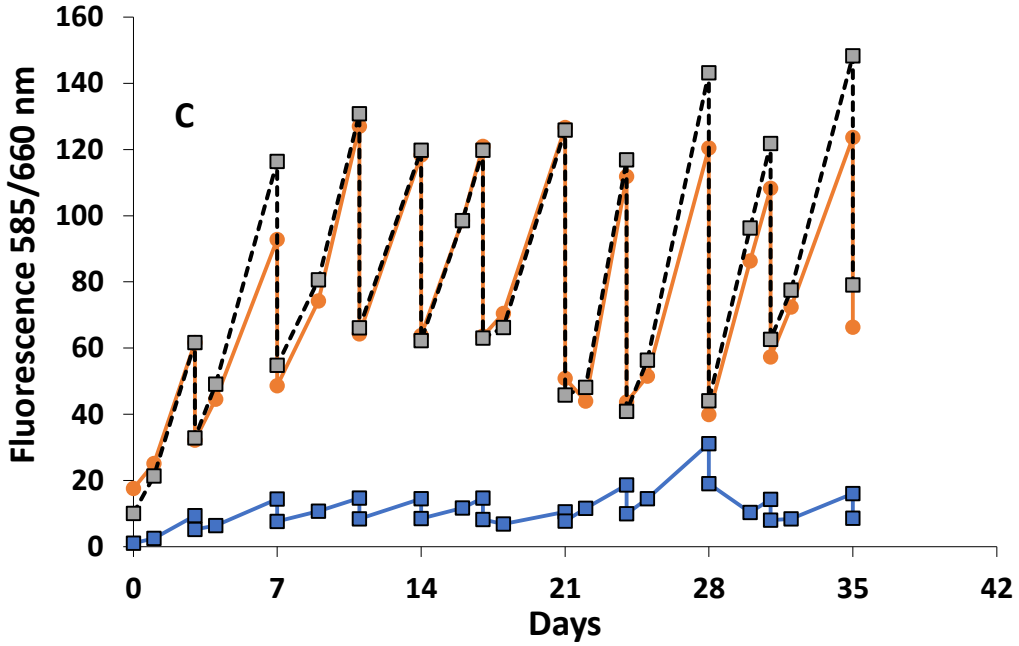

791

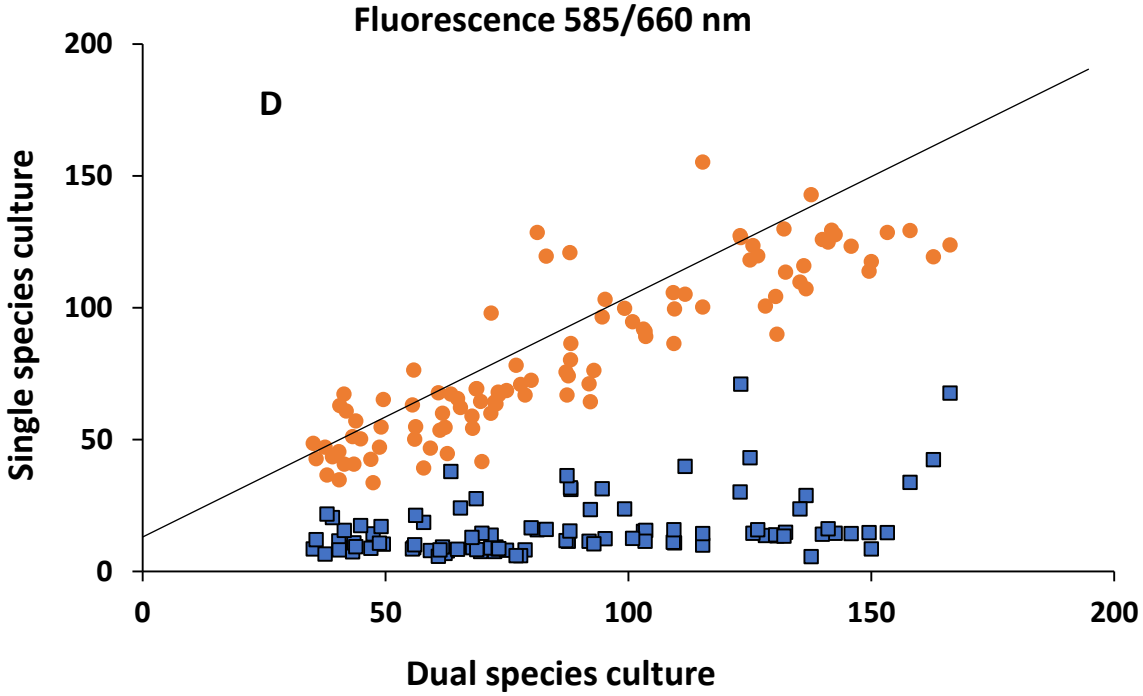

792

793

794

795

796 **Figure 8**

797

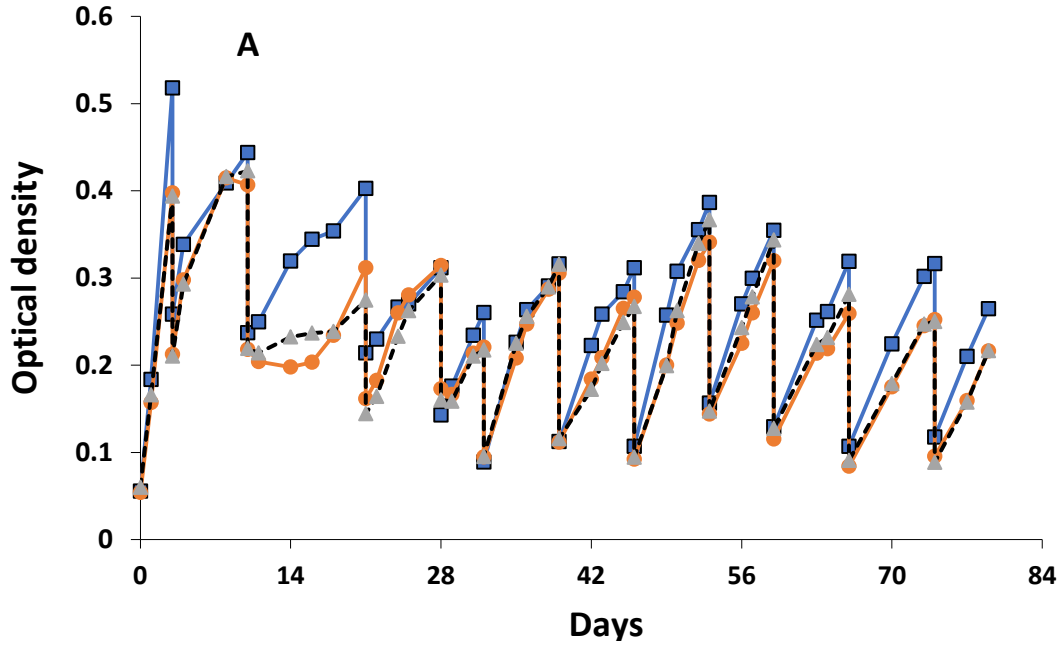

798

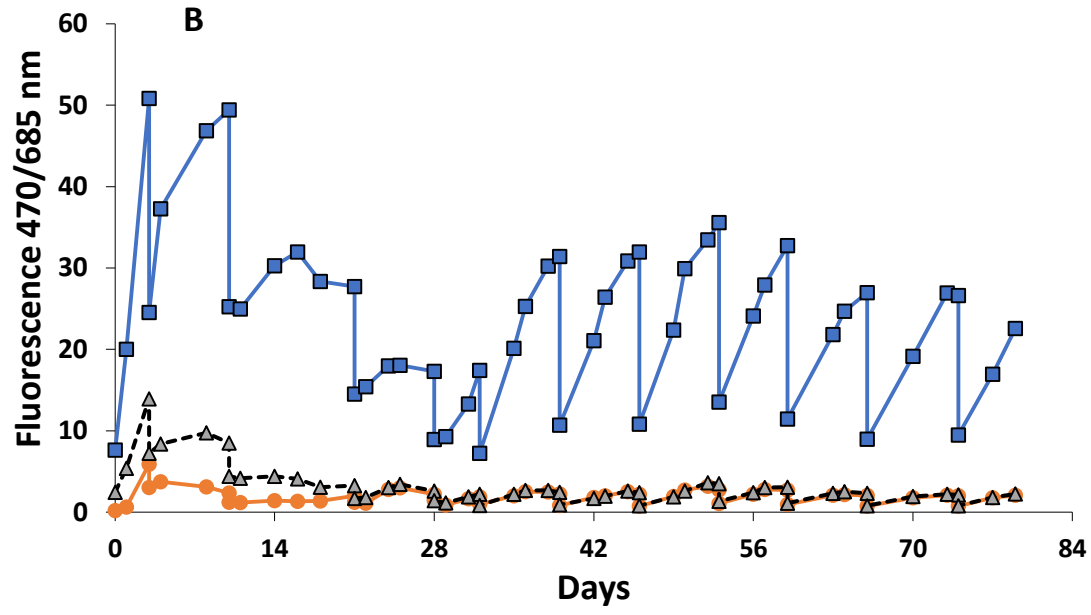

799

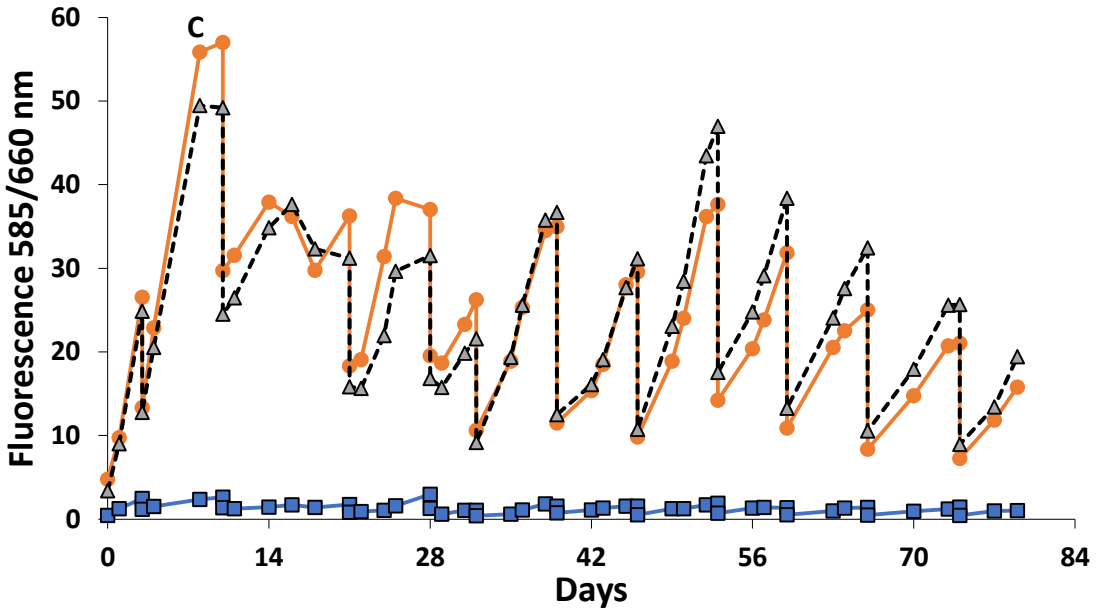
C
Fluorescence 585/660 nm
60
50
40
30
20
10
0
0
14
28
42
56
70
84
Days

800

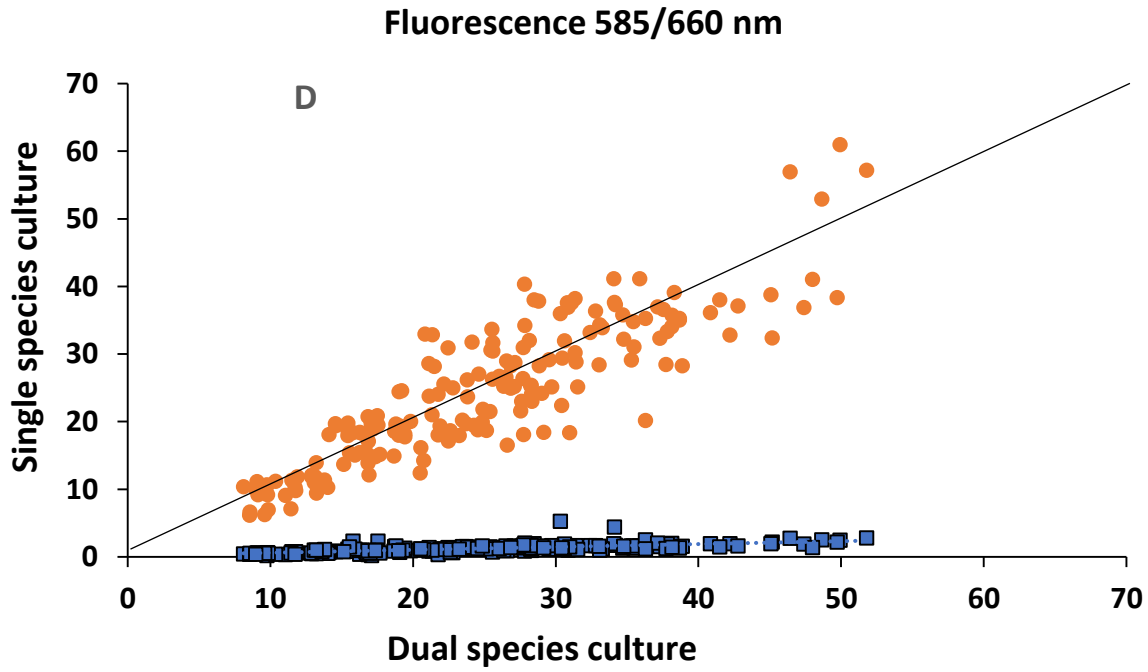
Fluorescence 585/660 nm
D
Single species culture
70
60
50
40
30
20
10
0
0
10
20
30
40
50
60
70
Dual species culture

801

802

803 **Figure 9**

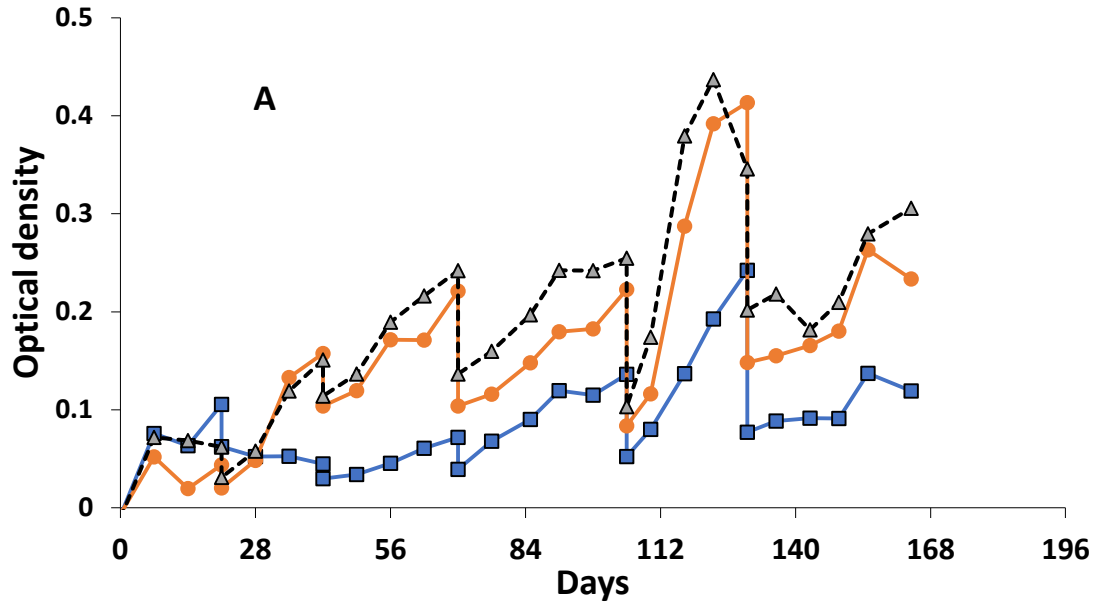

804

805

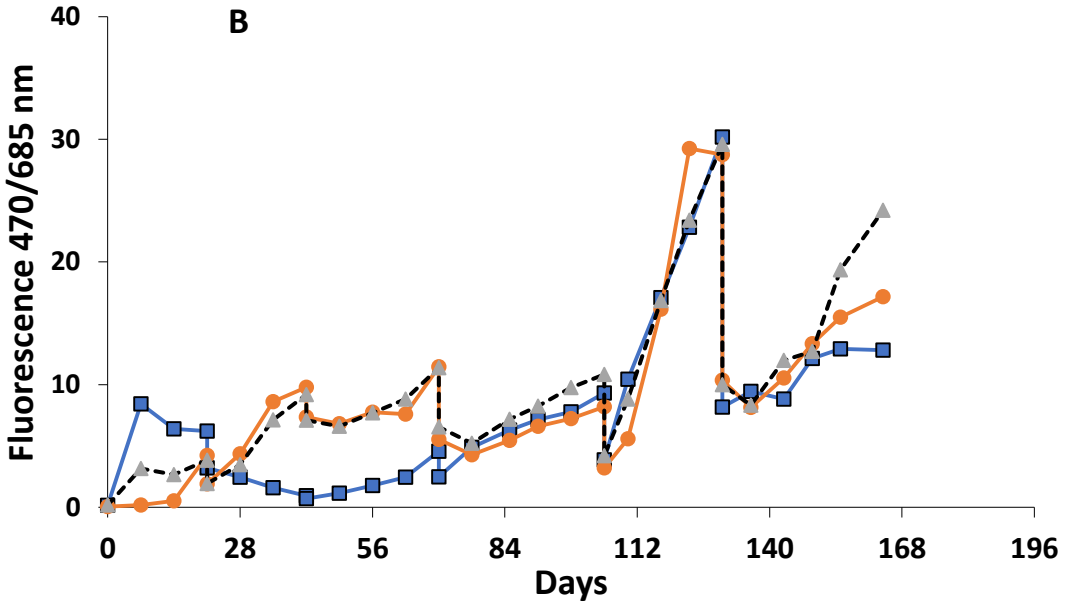

806

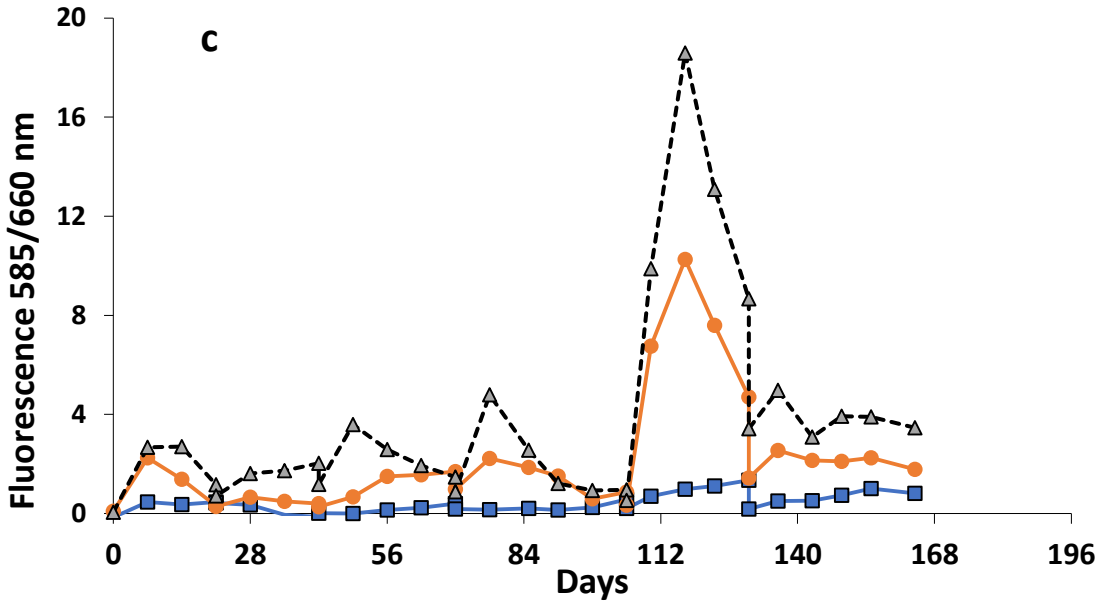
C
Fluorescence 585/660 nm
20
16
12
8
4
0
0
28
56
84
112
140
168
196
Days

807

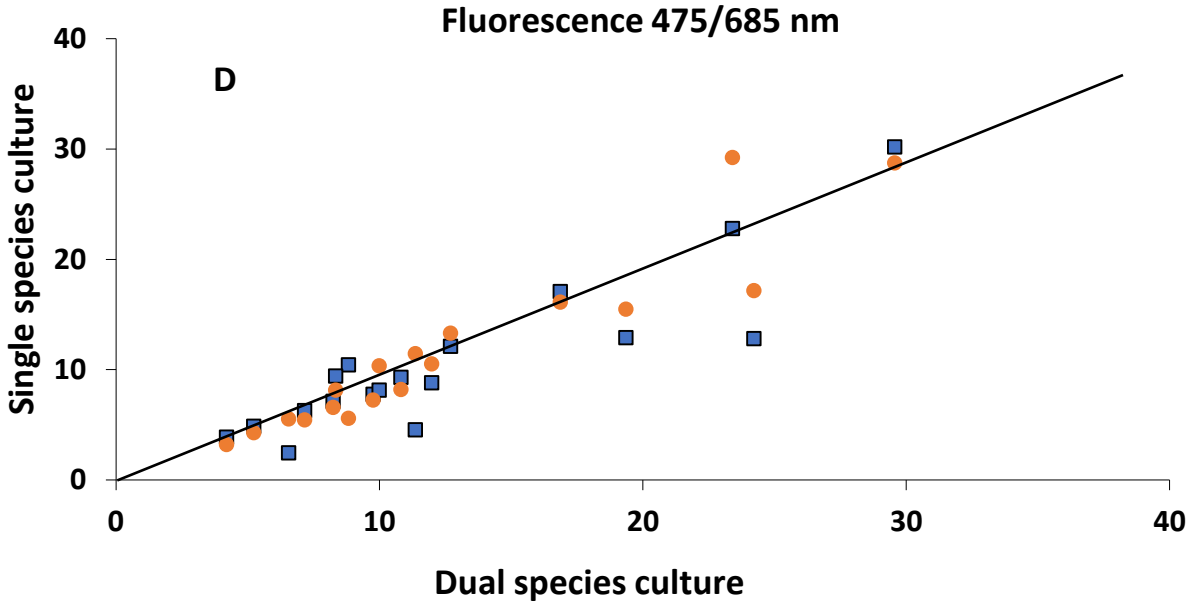
Fluorescence 475/685 nm
D
Single species culture
40
30
20
10
0
0
10
20
30
40
Dual species culture

808

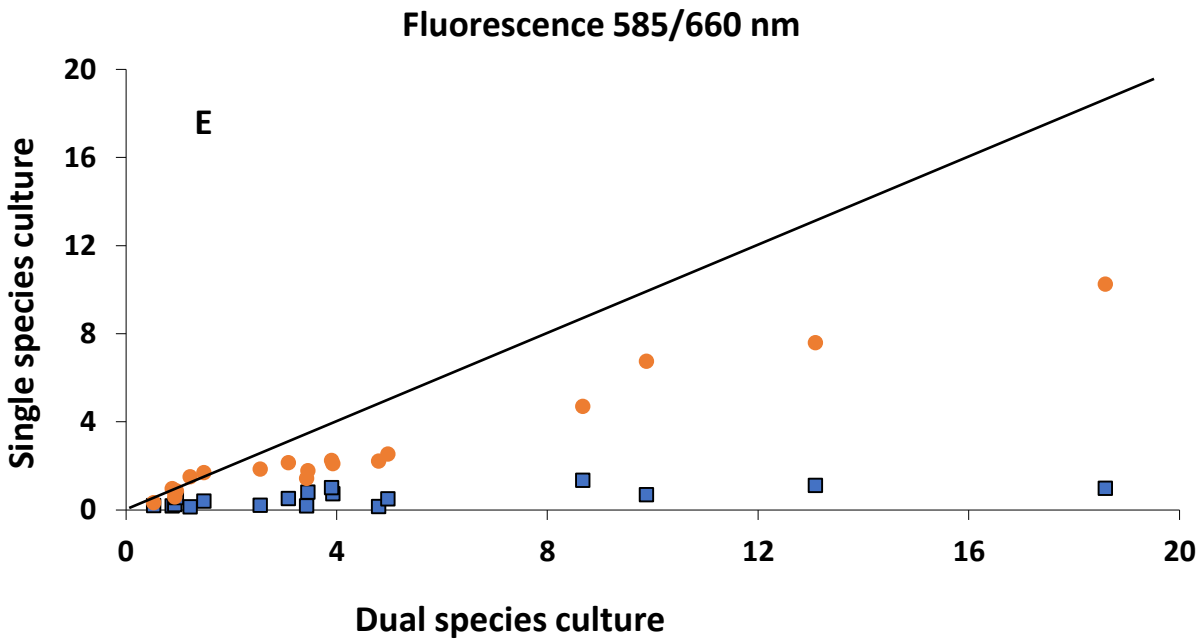
Fluorescence 585/660 nm
E
Single species culture
Dual species culture
0
4
8
12
16
20

809

810

SUPPORTING INFORMATION

TABLE S1 Final nutrient concentrations (μmol L^{-1}) in modified Bold 3N medium. Recipe on UTEX web site (https://utex.org/pages/algal-culture-media).

Nutrient	Chemical formulation	Nutrient concentration
Calcium	$CaCl_2.2H_2O$	170
Iron (total)	$FeCl_3.6H_2O$ plus Na_2EDTA (chelator)	0.0005, 0.05 and 0.5
Magnesium	$MgSO_4.7H_2O$	304
Nitrogen	$NaNO_3$	8,825
Phosphorus	K_2HPO_4 plus KH_2PO_4	172
Sulfate	$MgSO_4.7H_2O$ plus $CuSO_4.5H_2O$	304
Boron	H_3BO_3	46
Cobalt	$CoCl_2.6H_2O$	0.05
Copper	$CuSO_4.5H_2O$	0.19
Manganese	$MnCl_2.4H_2O$	1.24
Molybdenum	$Na_2MoO_4.2H_2O$	0.1
Zinc	$ZnCl_2$	0.22

TABLE S2 Nutrient concentrations (µmol L^{-1}) used to calculate free ferric (Fe^{+3}) in modified Bold 3N medium with Visual MINTEQ (v 3.1, beta).

Component	Concentration
Ca^{2+}	170
Cl^{-}	771
Co^{3+}	0.05
Cu^{2+}	0.19
EDTA	12
Total Fe	0.0005, 0.05, and 0.5
H_3BO_3	46
K^{+}	215
Mg^{2+}	304
Mn^{3+}	1.24
MoO_4^{2-}	0.1
Na^{+}	9277
NO_3^{-}	8825
O_2 (aq)	68
PO_4^{3-}	172
SO_4^{2-}	304
Zn^{+2}	0.22

FIGURE S1 Growth curves of the phytoplankton species over time at different Fe concentrations. Species labelled with (-N) indicates N-deplete. Lines are modelled growth curves using the logistic growth equation.

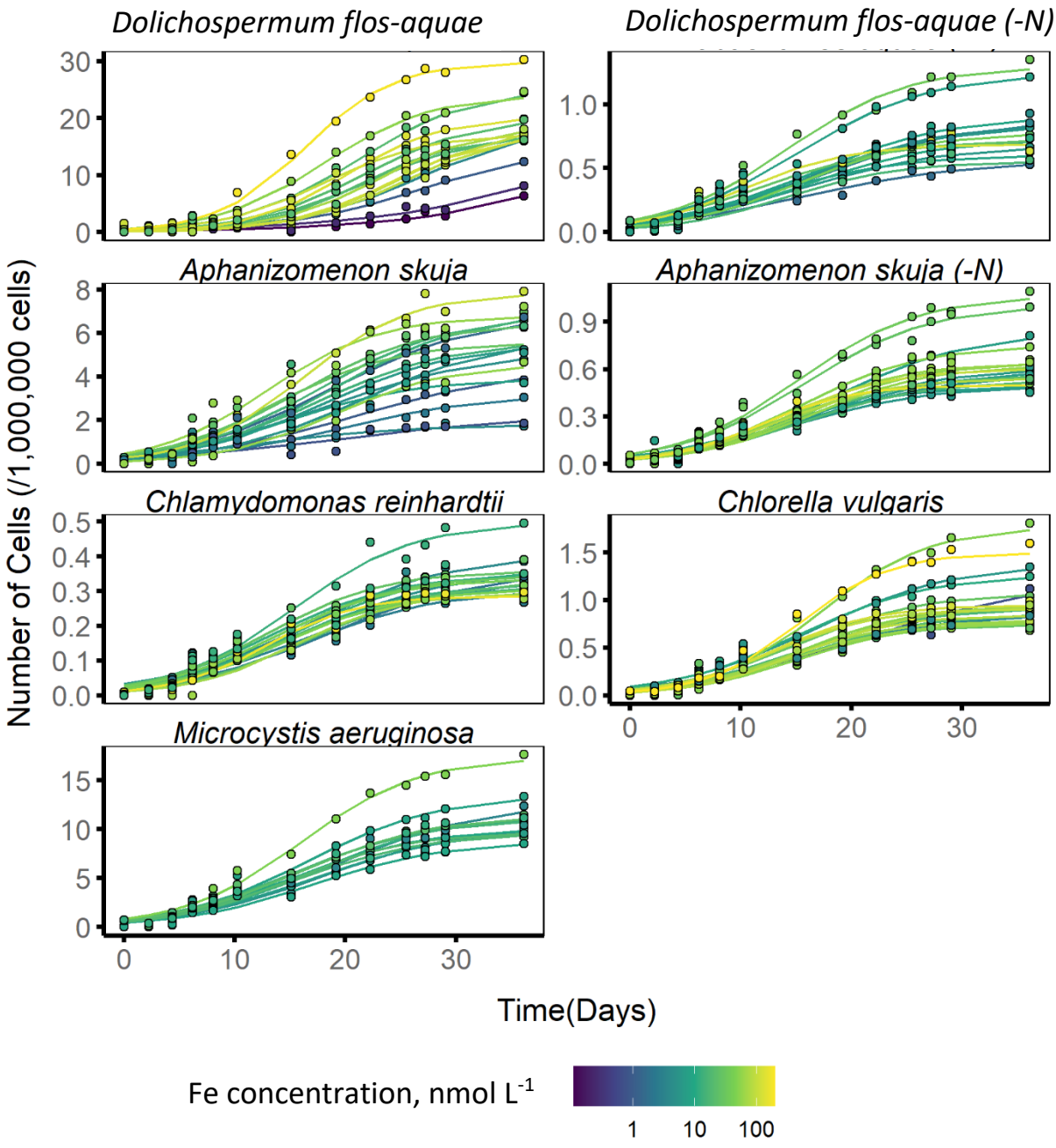

FIGURE S2 Boxplots displaying median, first and third quartiles, and range in growth rates (μ) for each species. Color gradation in observations indicate the Fe concentration. '-N' indicates N-deplete.